Genomic selection for genotype performance and stability using information on multiple traits and multiple environments

Genomic selection for genotype performance and stability using information on multiple traits and multiple environments

Jon Bančič (jbancic@ed.ac.uk)
The University of Edinburgh The Roslin Institute https://orcid.org/0000-0001-7077-7163
Ben Ovenden
NSW DPI: New South Wales Department of Primary Industries
Gregor Gorjanc
The University of Edinburgh The Roslin Institute
Daniel Tolhurst
The University of Edinburgh The Roslin Institute

Research Article

Keywords: Factor analytic model, Multi-environment trial data, Multi-trait data, Genotype by environment by trait interaction, Genomic selection, Selection index, Rice breeding

Posted Date: July 12th, 2022

DOI: https://doi.org/10.21203/rs.3.rs-1836102/v1

Genomic selection for genotype performance and stability using information on multiple traits and multiple environments

J. Bancic, B. Ovenden , G. Gorjanc, D.J. Tolhurst

Received: date / Accepted: date

Key message The inclusion of multiple traits and multiple environments within a partially separable factor analytic approach for genomic selection provides breeders with an informative framework to utilise genotype by environment by trait interaction for efficient selection across multiple traits.

Abstract This paper develops a single-stage genomic selection (GS) approach which incorporates information on multiple traits and multiple environments within a partially separable factor analytic framework. The factor analytic linear mixed model is an effective method for analysing multi-environment trial (MET) datasets, but is yet to be extended to GS for multiple traits and multiple environments. The advantage of incorporating all three sources of information is that breeders can utilise genotype by environment by trait interaction (GETI) to obtain more accurate predictions across correlated traits and environments. The partially separable factor analytic linear mixed model (SFA-LMM) developed in this paper is based on a three-way separable structure, with a factor analytic model for traits, a factor analytic model for environments and a genomic relationship matrix for genotypes. This structure is then modified to enable a different genotype by environment interaction (GEI) pattern for each trait, and a different genotype by trait interaction (GTI) pattern for each environment. The SFA-LMM is demonstrated on a multi-trait MET dataset from The Australian Rice Breeding Program. Selection within the rice breeding program is demonstrated using a selection index based on measures of genotype performance and stability. This approach represents an important continuation in the advancement of plant breeding analyses, particularly with the advent of high-throughput phenotypic datasets involving a very large number of traits and environments.

Keywords Factor analytic model · Multi-environment trial data · Multi-trait data · Genotype by environment by trait interaction · Genomic selection · Selection index · Rice breeding

J. Bancic ✉
The Roslin Institute and Royal (Dick) School of Veterinary Studies, University of Edinburgh, Easter Bush, Midlothian EH25 9RG, United Kingdom
E-mail: jon.bancic@ed.ac.uk

1 Introduction

This paper develops a single-stage genomic selection (GS) approach which incorporates information on multiple traits and multiple environments within a partially separable factor analytic framework. The single-trait approach of Smith et al. (2001) is an effective method for analysing multi-environment trial (MET) datasets which includes a factor analytic model for genotype by environment interaction (GEI). The factor analytic model has already been applied to multi-trait datasets to model genotype by trait interaction (GTI), but is yet to be extended to multiple traits as well as multiple environments (Meyer, 2007, 2009). The GS approach developed in this paper extends the factor analytic model to incorporate information on multiple traits and multiple environments. Selection is then demonstrated using an index based on measures of genotype performance and stability (Smith and Cullis, 2018).

In plant breeding, selection is based on genotype performance across a set of production environments for multiple traits of commercial importance. Traditionally, independent culling has been used by setting thresholds for each trait and selecting genotypes that meet the thresholds for all traits. However, it does not take into account the genetic correlations between traits and may also exclude genotypes that could serve as potential parents (e.g. high-yielding genotypes that are too tall for release). A more efficient approach is using a selection index, which takes into account the genetic correlations between traits and weights their importance based on the breeding objectives (Bernardo, 2010). Selection indices have become a popular approach to advance material through the breeding pipeline for commercial release as well as selecting potential parents.

Genomic selection is a form of marker-assisted selection that can improve the genetic gain in plant breeding programs (Meuwissen et al., 2001). GS has already been used in the context of a selection index (e.g., Slavov et al., 2019; Michel et al., 2019), however, many of the current applications only use information on multiple environments for a single trait or multiple traits for a single environment, and this may limit the potential genetic gain. The advantage of incorporating all three sources of information is that breeders can utilise genotype by environment by trait interaction (GETI), which is an impediment to efficient selection and reflects the differential response of genotypes to different environments and different traits. Another advantage is that breeders can obtain more accurate predictions across correlated traits and environments, regardless of whether there is phenotypic data available or not. This is especially appealing for i) traits and environments with low heritability or ii) traits that are difficult and/or expensive to phenotype.

Information on multiple traits and multiple environments was first considered for GS by Montesinos-López et al. (2016a). They presented a three-way separable model for GETI, which is represented by the Kronecker product of three variance matrices (see Appendix A). Their separable model includes an unstructured variance matrix for traits, a diagonal matrix for environments and a genomic relationship matrix for genotypes. Montesinos-López et al. (2019) extended this approach to include an unstructured variance matrix for environments as well as traits, however, they did not address spatial variation and other non-genetic sources (Gilmour et al., 1997). They also used a restrictive model for GETI which assumes the same GEI pattern for each trait and the same GTI pattern for each environment. These examples highlight the limitations of current approaches for analysing multi-trait MET datasets.

The approach of Smith et al. (2007) includes a model for GETI as well as non-genetic sources of variation. Their three-way separable model includes an unstructured variance matrix for traits and a factor analytic variance matrix for environments, but they only consider a diagonal matrix for genotypes. The factor analytic model provides a parsimonious alternative to the unstructured matrix, and has been widely adopted in many plant breeding programs (Ukrainetz et al., 2018). Recently, Smith et al. (2019) extended the approach of Smith et al. (2007) to include a less restrictive model for GETI which captures a different GEI pattern for each trait (treatment) and a different GTI pattern for each environment. They also demonstrated the application of plant breeding selection tools, where genotypes with high overall performance and stability are of high interest to breeders (Smith and Cullis, 2018). There are two limitations of their approach: i) the unstructured variance matrix becomes computationally prohibitive for a large number of traits and ii) they do not consider GS.

The aim of this paper is to extend the approach of Smith et al. (2019) for GS using a partially separable factor analytic model across multiple traits and multiple environments. This new approach is hereafter referred to as the partially separable factor analytic linear mixed model (SFA-LMM). The SFA-LMM was motivated by the need for:

1. *Dimension reduction* of high-throughput phenotypic datasets involving a very large number of traits and/or environments.
2. *Interpretability* of genotype by environment and genotype by trait interaction patterns.
3. *Efficient selection* using an index based on measures of genotype performance and stability, with common information shared across multiple traits and multiple environments.

The SFA-LMM is demonstrated on a multi-trait MET dataset from The Australian Rice Breeding Program.

2 Material and methods

2.1 Data description

The Australian Rice Breeding Program evaluates the commercial merit of test genotypes by annually conducting multi-environment field trials for multiple traits. There are four late-stages of field evaluation, which are pooled into S_1-S_2 and S_3-S_4 joint field trials. Note that only genotypes from stages S_3-S_4 are considered in this paper. Grain yield (YLD; t/ha), days to flowering (DTF) and plant height (PHT; cm) are the primary agronomic traits of commercial importance. The multi-trait MET dataset for stages S_3-S_4 and years 2017-18 is detailed below.

Experimental design

Table 1 presents a summary of the multi-trait MET dataset. A total of 291 rice genotypes were evaluated in 12 field trials across environments in the Murrumbidgee and Murray Valley rice growing regions of Australia (Figure 1). Each environment comprised a single trial, and is indexed by one of two years (2017 or 2018), one of two regions (Murrumbidgee or Murray Valley) and one of three growing seasons (early, mid or late). Each trial was designed as a randomised complete or incomplete (17MB_E) block design with 2-4 blocks of 36-84 genotypes for a total of 108-252 plots. Four check cultivars were evaluated in all 12 trials with phenotypes on 36 plots. Test genotypes were evaluated in 1-12 trials (mean of 3) with phenotypes recorded on 2-36 plots (mean of 8). The multi-trait MET dataset is therefore highly unbalanced between trials, and thence environments. Lastly, the mean yield and generalised narrow-sense heritability (Oakey et al., 2006) varied substantially between traits and environments.

Figure 2 presents a summary of the connectivity in the multi-trait MET dataset. The number of genotypes in common between environments ranged from 5 to 84, with mean of 19. The number of genotypes in common between years (102), regions (255) and seasons (27-36) produced good connectivity across these factors.

Multi-trait data

Table 2 presents a summary of the three agronomic traits; YLD, DTF and PHT. This table summarises the phenotypes for each year, region and season. All traits were recorded for all 291 genotypes in all 12 environments, except for missing plots. There are considerable differences between years, regions and seasons for all traits, but especially between regions for DTF and PHT and between seasons for YLD and DTF. The phenotypes for each trait were then scaled to unit variance for model fitting, with model parameters transformed back to their original scale for interpretation.

Marker data

Marker data were available for 266 (of the 291) genotypes and generated from DArTseq (Sansaloni et al., 2011), coded according to a high confidence set of 14,800 single-nucleotide polymorphisms (SNPs). The frequency of heterozygous markers was low given the level of selfing accumulated up to the S_3-S_4 stages. Monomorphic markers were then removed and missing markers were imputed using the k-nearest neighbour approach of Troyanskaya et al. (2001) with $k = 10$.

The genomic relationship matrix was constructed using the *pedicure* package (Butler, 2019) in *R* (R Core Team, 2021) according to VanRaden (2008) method 1. The default settings in *pedicure* were used as filters, with minor allele frequency $> 0.002\%$ and missing marker frequency $< 0.998\%$. A total of $11,845$ markers were retained using this criteria. The diagonal elements of the genomic relationship matrix ranged from 0.861 to 6.590, with mean of 1.825. The off-diagonals ranged from -0.822 to 2.492, with mean of -0.007.

2.2 Statistical models

Preliminaries

Assume the multi-trait MET dataset comprises $s = 3$ traits, $p = 12$ field trials (environments), $v = 266$ genotypes and $r = 11,845$ markers for $n = 2,358$ plots in total. Also assume the ns-vector of scaled phenotypic data is given by $\mathbf{y} = (\mathbf{y}_1^\top, \mathbf{y}_2^\top, \ldots, \mathbf{y}_s^\top)^\top$, where $\mathbf{y}_i = (\mathbf{y}_{i;1}^\top, \mathbf{y}_{i;2}^\top, \ldots, \mathbf{y}_{i;p}^\top)^\top$ is the n-vector of scaled data for trait i and $\mathbf{y}_{i;j}$ is the n_j-vector of data for trait i and environment j. The length of $\mathbf{y}$ is therefore given by:

$$ns = \sum_{i=1}^{s}\sum_{j=1}^{p} n_j = \sum_{i=1}^{s} n,$$

where n_j is the length of $\mathbf{y}_{i;j}$ and n is the length of $\mathbf{y}_i$.

Linear mixed model

The linear mixed model for $\mathbf{y}$ can be written as:

$$\mathbf{y} = \mathbf{X}\boldsymbol{\tau} + (\mathbf{I}_s \otimes \mathbf{Z})\mathbf{u} + (\mathbf{I}_s \otimes \mathbf{Z}_\mathbf{p})\mathbf{u}_\mathbf{p} + \mathbf{e}, \tag{1}$$

where $\boldsymbol{\tau}$ is a vector of fixed effects with associated design matrix $\mathbf{X}$ (assumed to have full column rank); $\mathbf{u}$ is a vps-vector of random *genotype by environment by trait* (GET) effects with $n \times vp$ design matrix $\mathbf{Z}$, $\mathbf{u}_\mathbf{p}$ is a vector of random non-genetic (peripheral) effects with design matrix $\mathbf{Z}_\mathbf{p}$ and $\mathbf{e}$ is the ns-vector of residuals. Note that $\otimes$ is the Kronecker product operator used to construct separable structures (see Appendix A).

The vector of fixed effects, $\boldsymbol{\tau}$, includes the mean parameter for each trait, environment and their interaction. The vector of random non-genetic effects, $\mathbf{u}_\mathbf{p}$, includes the plot structures of each environment within

each trait (Bailey, 2008). Further effects in $\boldsymbol{\tau}$ and $\mathbf{u_p}$ may relate to genotypes without marker data (Tolhurst et al., 2019) and spatial modelling (Gilmour et al., 1997), respectively.

It is assumed that:

$$\begin{bmatrix} \mathbf{u} \\ \mathbf{u_p} \\ \mathbf{e} \end{bmatrix} \sim \mathrm{N}\left(\begin{bmatrix} \mathbf{0} \\ \mathbf{0} \\ \mathbf{0} \end{bmatrix}, \begin{bmatrix} \mathbf{G} & \mathbf{0} & \mathbf{0} \\ \mathbf{0} & \mathbf{G_p} & \mathbf{0} \\ \mathbf{0} & \mathbf{0} & \mathbf{R} \end{bmatrix} \right), \tag{2}$$

where $\mathbf{G_p} = \oplus_{h=1}^{ps} \mathbf{G}_{\mathbf{p}_h}$ is diagonal with a separate variance component model for each trait by environment combination and $\oplus$ is the direct sum operator. More parsimonious forms of $\mathbf{G_p}$ can be used, including those which assume separability between traits and environments. The form of $\mathbf{G}$ and $\mathbf{R}$ is developed below.

2.3 Models for the residuals

The two models considered for the residuals are based on either a non-separable or separable structure (see Appendix A). The non-separable residual model is given by $\mathbf{R} = \oplus_{h=1}^{ps} \mathbf{R}_h$, which is block diagonal with a separate spatial model for each trait by environment combination. The separable residual model is given by:

$$\mathbf{R} = \mathbf{R_t} \otimes \mathbf{R_e} \tag{3}$$

where $\mathbf{R_t}$ is a $s \times s$ unstructured variance matrix between traits and $\mathbf{R_e} = \oplus_{j=1}^{p} \mathbf{R}_{\mathbf{e}_j}$ is a $n \times n$ block diagonal variance matrix with a separate spatial model for each environment. More parsimonious forms of $\mathbf{R_t}$ can be used, including reduced rank factor analytic models (Faveri et al., 2017). The spatial model for environment j is given by (Gilmour et al., 1997):

$$\mathbf{R}_{\mathbf{e}_j} = \sigma^2_{r_j} \boldsymbol{\Sigma}_{\mathbf{c}_j}(\rho_{c_j}) \otimes \boldsymbol{\Sigma}_{\mathbf{r}_j}(\rho_{r_j}), \tag{4}$$

where $\boldsymbol{\Sigma}_{\mathbf{c}_j}$ and $\boldsymbol{\Sigma}_{\mathbf{r}_j}$ are $c_j \times c_j$ and $r_j \times r_j$ correlation matrices which comprise a single column and row auto-correlation parameter for the j^{th} environment, respectively.

The model in Equation 3 is restrictive since it assumes the same residual correlation between traits for all environments. This model can be modified to enable a different correlation between traits, with:

$$\mathbf{R} = \mathbf{R_t} \otimes \mathbf{R_e} + \boldsymbol{\Sigma}_\mathbf{t} \otimes \mathbf{I}_n + \mathbf{I}_s \otimes \boldsymbol{\Sigma}_\mathbf{e}, \tag{5}$$

where $\boldsymbol{\Sigma}_\mathbf{t} = \oplus_{i=1}^{s} \sigma^2_{t_i}$ and $\boldsymbol{\Sigma}_\mathbf{e} = \oplus_{j=1}^{p} \sigma^2_{e_i} \mathbf{I}_{n_j}$ are $s \times s$ and $n \times n$ diagonal variance matrices between traits and plots within environments, respectively. The variances, $\sigma^2_{t_i}$ and $\sigma^2_{e_j}$, capture any remaining random error specific to individual traits and environments, respectively. Note that the model in Equation 5 is no longer completely separable.

2.4 Model for the GET effects

Extending Oakey et al. (2007), the GET effects are partitioned into *additive* and *non-additive* GET effects, with:

$$\mathbf{u} = \mathbf{u_a} + \mathbf{u_n} \qquad \text{and} \qquad \mathbf{G} = \mathbf{G_a} + \mathbf{G_n}. \tag{6}$$

The form of the additive genetic variance matrix, $\mathbf{G_a}$, is developed below. The non-additive genetic variance matrix is given by $\mathbf{G_n} = \oplus_{h=1}^{ps} \mathbf{G}_{\mathbf{n}_h}$, which is diagonal with a separate variance component for each trait by environment combination. Other forms of $\mathbf{G_n}$ can be used where appropriate.

Model for the additive GET effects

Extending Stranden and Garrick (2009), the additive GET effects are modelled using marker data, with:

$$\begin{aligned} \mathbf{u_a} = (\mathbf{I}_{ps} \otimes \mathbf{M})\mathbf{u_m} \qquad \text{and} \qquad \mathbf{G_a} &= \mathbf{G_{te}} \otimes \mathbf{M}\mathbf{M}^\top / m \\ &= \mathbf{G_{te}} \otimes \mathbf{G_g} \end{aligned} \tag{7}$$

where $\mathbf{M} = [\mathbf{m}_1 \ \mathbf{m}_2 \ \ldots \ \mathbf{m}_r]$ is a $v \times r$ design matrix with columns given by the centred genotype scores for each marker, $\mathbf{u_m}$ is a rps-vector of additive marker by environment by trait effects, $\mathbf{G_{te}}$ is a $ps \times ps$ variance matrix between environments within traits and $\mathbf{G_g} = \mathbf{M}\mathbf{M}^\top / m$ is the $v \times v$ genomic relationship matrix between genotypes (VanRaden, 2008). The two forms of $\mathbf{G_{te}}$ considered below are based on either a non-separable or separable factor analytic model (see Appendix A).

2.5 Non-separable factor analytic (NFAk) model

The non-separable factor analytic model postulates the covariances between additive GET effects in terms of a small number, k, of latent common factors. The NFAk model for the additive GET effects is given by:

$$\begin{aligned} \mathbf{u_a} &= (\boldsymbol{\lambda}_1 \otimes \mathbf{I}_v)\mathbf{f}_1 + \ldots + (\boldsymbol{\lambda}_k \otimes \mathbf{I}_v)\mathbf{f}_k + \boldsymbol{\delta} \\ &= (\boldsymbol{\Lambda} \otimes \mathbf{I}_v)\mathbf{f} + \boldsymbol{\delta}, \end{aligned} \tag{8}$$

where $\boldsymbol{\Lambda} = \left[\boldsymbol{\lambda}_1 \, \boldsymbol{\lambda}_2 \, \ldots \, \boldsymbol{\lambda}_k\right]$ is a $ps \times k$ matrix of trait by environmental loadings, $\mathbf{f} = \left(\mathbf{f}_1^\top, \mathbf{f}_2^\top, \ldots, \mathbf{f}_k^\top\right)^\top$ is a vk-vector of genotype scores in which $\mathbf{f}_l$ is the v-vector for the l^{th} latent factor and $\boldsymbol{\delta} = (\boldsymbol{\delta}_{1;1}^\top, \boldsymbol{\delta}_{1;2}^\top, \ldots, \boldsymbol{\delta}_{p;s}^\top)^\top$ is a vps-vector of residual GET effects in which $\boldsymbol{\delta}_{i;j}$ is the v-vector specific to the i^{th} trait and j^{th} environment.

It is assumed that:

$$\begin{bmatrix} \mathbf{f} \\ \boldsymbol{\delta} \end{bmatrix} \sim \mathrm{N}\left(\begin{bmatrix} \mathbf{0} \\ \mathbf{0} \end{bmatrix}, \begin{bmatrix} \mathbf{I}_k & \mathbf{0} \\ \mathbf{0} & \boldsymbol{\Psi} \end{bmatrix} \otimes \mathbf{G_g} \right),$$

where $\boldsymbol{\Psi} = \oplus_{i=1}^{s} \oplus_{j=1}^{p} \psi_{i;j}$ is a $ps \times ps$ diagonal matrix in which $\psi_{i;j}$ is the additive specific variance for the i^{th} trait and j^{th} environment.

The NFAk variance matrix is therefore given by:

$$\mathbf{G_a} = \left(\boldsymbol{\Lambda}\boldsymbol{\Lambda}^\top + \boldsymbol{\Psi}\right) \otimes \mathbf{G_g}. \tag{9}$$

This variance matrix is an extension of the conventional factor analytic variance matrix of Smith et al. (2001) for GS for multiple traits and multiple environments.

2.6 Partially separable factor analytic models

Two partially separable models are also considered for the additive GET effects. These models are initially based on a separable variance structure between traits and environments, that is $\mathbf{G_{te}} = \mathbf{G_t} \otimes \mathbf{G_e}$. The variance matrix in Equation 7 can therefore be written as a three-way separable structure, with:

$$\mathbf{G_a} = \mathbf{G_t} \otimes \mathbf{G_e} \otimes \mathbf{G_g}, \tag{10}$$

where $\mathbf{G_t}$ is a $s \times s$ variance matrix between traits and $\mathbf{G_e}$ is a $p \times p$ variance matrix between environments. The two models then modify Equation 10 so that they cannot be represented by the Kronecker product of three variances matrices, and is thence referred to as partially separable. The main difference between the two partially separable models is that the trait dimension is based on either an unstructured model or factor analytic model.

Unstructured factor analytic (UFAk_e) model

Smith et al. (2019) proposed an unstructured variance model for traits and a factor analytic model for environments based on k_e latent factors. The UFAk_e model for the additive GET effects is given by:

$$\begin{aligned}\mathbf{u_a} &= (\mathbf{I}_s \otimes \boldsymbol{\lambda}_{\mathbf{e}_1} \otimes \mathbf{I}_v)\mathbf{f}_{\mathbf{e}_1} + \ldots + (\mathbf{I}_s \otimes \boldsymbol{\lambda}_{\mathbf{e}_{k_e}} \otimes \mathbf{I}_v)\mathbf{f}_{\mathbf{e}_{k_e}} + \boldsymbol{\delta_t} \\ &= (\mathbf{I}_s \otimes \boldsymbol{\Lambda_e} \otimes \mathbf{I}_v)\mathbf{f_e} + \boldsymbol{\delta_t}\end{aligned} \tag{11}$$

where $\boldsymbol{\Lambda_e} = \left[\boldsymbol{\lambda}_{\mathbf{e}_1}\ \boldsymbol{\lambda}_{\mathbf{e}_2}\ \ldots\ \boldsymbol{\lambda}_{\mathbf{e}_{k_e}}\right]$ is a $p \times k_e$ matrix of environmental loadings, $\mathbf{f_e} = \left(\mathbf{f}_{\mathbf{e}_1}^\top, \mathbf{f}_{\mathbf{e}_2}^\top, \ldots, \mathbf{f}_{\mathbf{e}_{k_e}}^\top\right)^\top$ is a vk_e-vector of genotype scores in which $\mathbf{f}_{\mathbf{e}_l}$ is the v-vector for the l^{th} latent factor and $\boldsymbol{\delta_t} = (\boldsymbol{\delta}_{\mathbf{t}_1}^\top, \boldsymbol{\delta}_{\mathbf{t}_2}^\top, \ldots, \boldsymbol{\delta}_{\mathbf{t}_s}^\top)^\top$ is the vps-vector of residual GET effects in which $\boldsymbol{\delta}_{\mathbf{t}_i}$ is the vp-vector across environments specific to the i^{th} trait.

It is assumed that:

$$\begin{bmatrix}\mathbf{f_e} \\ \boldsymbol{\delta_t}\end{bmatrix} \sim \mathrm{N}\left(\begin{bmatrix}\mathbf{0} \\ \mathbf{0}\end{bmatrix}, \begin{bmatrix}\boldsymbol{\Sigma_t} \otimes \mathbf{I}_{k_e} & \mathbf{0} \\ \mathbf{0} & \boldsymbol{\Psi_t} \otimes \mathbf{I}_p\end{bmatrix} \otimes \mathbf{G_g}\right),$$

where $\boldsymbol{\Sigma_t}$ is a $s \times s$ unstructured variance matrix across traits and $\boldsymbol{\Psi_t} = \oplus_{i=1}^{s} \psi_{t_i}$ is a diagonal matrix in which ψ_{t_i} is the additive specific variance for the i^{th} trait.

The UFAk_e variance matrix is therefore given by:

$$\mathbf{G_a} = \left(\boldsymbol{\Sigma_t} \otimes \boldsymbol{\Lambda_e}\boldsymbol{\Lambda_e}^\top + \boldsymbol{\Psi_t} \otimes \mathbf{I}_p\right) \otimes \mathbf{G_g}. \tag{12}$$

Partially separable factor analytic (SFAk_t-k_e) model

The partially separable factor analytic model developed below is a parsimonious alternative to the UFAk_e model. This model postulates the covariances between additive GET effects in terms of a small number, k_t and k_e, of latent trait and environmental factors, respectively. The SFAk_t-k_e variance matrix is given by:

$$\mathbf{G_a} = (\boldsymbol{\Lambda_t}\boldsymbol{\Lambda_t}^\top + \boldsymbol{\Psi_t}) \otimes (\boldsymbol{\Lambda_e}\boldsymbol{\Lambda_e}^\top + \boldsymbol{\Psi_e}) \otimes \mathbf{G_g}, \tag{13}$$

with trait and environmental loadings given by:

$$\boldsymbol{\Lambda_t} = \left[\boldsymbol{\lambda}_{\mathbf{t}_1}\ \boldsymbol{\lambda}_{\mathbf{t}_2}\ \ldots\ \boldsymbol{\lambda}_{\mathbf{t}_{k_t}}\right] \quad \text{and} \quad \boldsymbol{\Lambda_e} = \left[\boldsymbol{\lambda}_{\mathbf{e}_1}\ \boldsymbol{\lambda}_{\mathbf{e}_2}\ \ldots\ \boldsymbol{\lambda}_{\mathbf{e}_{k_e}}\right],$$

which are $s \times k_t$ and $p \times k_e$ matrices, respectively, where $\boldsymbol{\lambda}_{\mathbf{t}_l}$ is an s-vector for the l_t^{th} trait factor and $\boldsymbol{\lambda}_{\mathbf{e}_l}$ is a p-vector for the l_e^{th} environmental factor. Note that this formulation enables a different order for the trait and environmental factors, that is k_t and k_e.

The specific variances are given by:

$$\boldsymbol{\Psi_t} = \oplus_{i=1}^{s}\psi_{t_i} \qquad \text{and} \qquad \boldsymbol{\Psi_e} = \oplus_{j=1}^{p}\psi_{e_j}, \tag{14}$$

which are $s \times s$ and $p \times p$ diagonal matrices for traits and environments, respectively, where ψ_{t_i} is the additive specific variance for the i^{th} trait and ψ_{e_j} is the additive specific variance for the j^{th} environment.

The model in Equation 13 is restrictive since it assumes the same GEI pattern for each trait and the same GTI pattern for each environment (see Appendix A). This model can be modified to enable different GEI and GTI patterns, with:

$$\mathbf{G_a} = (\boldsymbol{\Lambda_t}\boldsymbol{\Lambda_t}^\top \otimes \boldsymbol{\Lambda_e}\boldsymbol{\Lambda_e}^\top + \boldsymbol{\Psi_t} \otimes \mathbf{I}_p + \mathbf{I}_s \otimes \boldsymbol{\Psi_e}) \otimes \mathbf{G_g}. \tag{15}$$

The SFAk_t-k_e model for the additive GET effects is therefore given by:

$$\begin{aligned}\mathbf{u_a} &= (\boldsymbol{\lambda}_{\mathbf{t}_1} \otimes \boldsymbol{\lambda}_{\mathbf{e}_1} \otimes \mathbf{I}_v)\mathbf{f}_{\mathbf{te}_1} + \ldots + \\ &\quad (\boldsymbol{\lambda}_{\mathbf{t}_{k_t}} \otimes \boldsymbol{\lambda}_{\mathbf{e}_{k_e}} \otimes \mathbf{I}_v)\mathbf{f}_{\mathbf{te}_{k_t k_e}} + \boldsymbol{\delta_t} + \boldsymbol{\delta_e} \\ &= (\boldsymbol{\Lambda_t} \otimes \boldsymbol{\Lambda_e} \otimes \mathbf{I}_v)\mathbf{f_{te}} + \boldsymbol{\delta_t} + \boldsymbol{\delta_e}\end{aligned} \tag{16}$$

where $[\boldsymbol{\Lambda_t} \otimes \boldsymbol{\Lambda_e}]$ is a $ps \times k_t k_e$ matrix of joint factor loadings across traits and environments and $\mathbf{f_{te}} = \left(\mathbf{f}_{\mathbf{te}_{1;1}}^\top, \mathbf{f}_{\mathbf{te}_{1;2}}^\top, \ldots, \mathbf{f}_{\mathbf{te}_{k_t;k_e}}^\top\right)^\top$ is a vk_tk_e-vector of genotype scores in which $\mathbf{f}_{\mathbf{te}_{l_t;l_e}}$ is the v-vector for the l_t^{th} trait and l_e^{th} environmental factor. The vps-vectors of residual GET effects are given by:

$$\boldsymbol{\delta_t} = (\boldsymbol{\delta}_{\mathbf{t}_1}^\top, \boldsymbol{\delta}_{\mathbf{t}_2}^\top, \ldots, \boldsymbol{\delta}_{\mathbf{t}_s}^\top)^\top \quad \text{and} \quad \boldsymbol{\delta_e} = (\boldsymbol{\delta}_{\mathbf{e}_1}^\top, \boldsymbol{\delta}_{\mathbf{e}_2}^\top, \ldots, \boldsymbol{\delta}_{\mathbf{e}_p}^\top)^\top,$$

where $\boldsymbol{\delta}_{\mathbf{t}_i}$ is a vp-vector across environments specific to the i^{th} trait and $\boldsymbol{\delta}_{\mathbf{e}_j}$ is a vs-vector across traits specific to the j^{th} environment.

Lastly, it is assumed that:

$$\begin{bmatrix}\mathbf{f_{te}} \\ \boldsymbol{\delta_t} \\ \boldsymbol{\delta_e}\end{bmatrix} \sim \mathrm{N}\left(\begin{bmatrix}\mathbf{0} \\ \mathbf{0} \\ \mathbf{0}\end{bmatrix}, \begin{bmatrix}\mathbf{I}_{k_t} \otimes \mathbf{I}_{k_e} & \mathbf{0} & \mathbf{0} \\ \mathbf{0} & \boldsymbol{\Psi_t} \otimes \mathbf{I}_p & \mathbf{0} \\ \mathbf{0} & \mathbf{0} & \mathbf{I}_s \otimes \boldsymbol{\Psi_e}\end{bmatrix} \otimes \mathbf{G_g}\right),$$

where $\boldsymbol{\Psi_t}$ and $\boldsymbol{\Psi_e}$ are defined in Equation 14.

2.7 Model estimation

All models presented above were implemented within a linear mixed model obtained by substituting Equation 6 into Equation 1, which gives:

$$\mathbf{y} = \mathbf{X}\boldsymbol{\tau} + (\mathbf{I}_s \otimes \mathbf{Z})(\mathbf{u_a} + \mathbf{u_n}) + (\mathbf{I}_s \otimes \mathbf{Z_p})\,\mathbf{u_p} + \mathbf{e}. \tag{17}$$

The non-separable factor analytic linear mixed model (NFA-LMM) is then obtained by substituting Equation 8 into Equation 17, which gives:

$$\begin{aligned}\mathbf{y} = \mathbf{X}\boldsymbol{\tau} + \mathbf{Z}_{\boldsymbol{\Lambda}}\mathbf{f} + (\mathbf{I}_s \otimes \mathbf{Z})\boldsymbol{\delta} + (\mathbf{I}_s \otimes \mathbf{Z})\,\mathbf{u_n} + \\ (\mathbf{I}_s \otimes \mathbf{Z_p})\,\mathbf{u_p} + \mathbf{e},\end{aligned} \tag{18}$$

where $\mathbf{Z}_{\mathbf{\Lambda}} = (\mathbf{I}_s \otimes \mathbf{Z})[\mathbf{\Lambda} \otimes \mathbf{I}_v]$. In this model, the covariances between GET effects are based on a non-separable factor analytic model between traits and environments.

The unstructured factor analytic linear mixed model (UFA-LMM) is obtained by substituting Equation 11 into Equation 17, which gives:

$$\mathbf{y} = \mathbf{X}\boldsymbol{\tau} + \mathbf{Z}_{\mathbf{\Lambda_e}}\mathbf{f_e} + (\mathbf{I}_s \otimes \mathbf{Z})\,\boldsymbol{\delta}_\mathbf{t} + (\mathbf{I}_s \otimes \mathbf{Z})\,\mathbf{u_n} + (\mathbf{I}_s \otimes \mathbf{Z_p})\,\mathbf{u_p} + \mathbf{e}, \tag{19}$$

where $\mathbf{Z}_{\mathbf{\Lambda_e}} = \mathbf{I}_s \otimes \mathbf{Z}[\mathbf{\Lambda_e} \otimes \mathbf{I}_v]$. In this model, the covariances between GET effects are based on an unstructured factor analytic model between traits and environments.

The partially separable factor analytic linear mixed model (SFA-LMM) is obtained by substituting Equation 16 into Equation 17, which gives:

$$\mathbf{y} = \mathbf{X}\boldsymbol{\tau} + \mathbf{Z}_{\mathbf{\Lambda_{te}}}\mathbf{f_{te}} + (\mathbf{I}_s \otimes \mathbf{Z})\,(\boldsymbol{\delta}_\mathbf{t} + \boldsymbol{\delta}_\mathbf{e}) + (\mathbf{I}_s \otimes \mathbf{Z})\,\mathbf{u_n} + (\mathbf{I}_s \otimes \mathbf{Z_p})\,\mathbf{u_p} + \mathbf{e}, \tag{20}$$

where $\mathbf{Z}_{\mathbf{\Lambda_{te}}} = \mathbf{\Lambda_t} \otimes \mathbf{Z}[\mathbf{\Lambda_e} \otimes \mathbf{I}_v]$. In this model, the covariances between GET effects are based on a partially separable factor analytic model between traits and environments.

All linear mixed models were fitted in *R* (R Core Team, 2021) using `ASReml-R` (Butler et al., 2017). `ASReml-R` obtains residual maximum likelihood (REML) estimates of the variance parameters using an extension of the average information algorithm (Gilmour et al., 1995). The REML estimates of the key variance parameters are given by $\left[\hat{\mathbf{\Lambda}}_\mathbf{t} \otimes \hat{\mathbf{\Lambda}}_\mathbf{e}\right]$, $\hat{\mathbf{\Psi}}_\mathbf{t}$ and $\hat{\mathbf{\Psi}}_\mathbf{e}$. Note that constraints are required to ensure a unique solution for $\left[\hat{\mathbf{\Lambda}}_\mathbf{t} \otimes \hat{\mathbf{\Lambda}}_\mathbf{e}\right]$ (see Appendix B). The empirical BLUPs of the key random effects are then given by $\tilde{\mathbf{f}}_\mathbf{te}$, $\tilde{\boldsymbol{\delta}}_\mathbf{t}$ and $\tilde{\boldsymbol{\delta}}_\mathbf{e}$. Lastly, note that the phenotypes for each trait were scaled to unit variance during estimation to assist convergence. The variance parameters and random effects were then transformed back to their original scale after estimation.

2.8 Model selection

Model selection was achieved using a combination of formal and informal criteria. Formal assessment was achieved using the Akaike Information Criterion (AIC). Informal assessment was achieved using the percentage of additive genetic variance explained by the trait and environmental factors. There are three measures for the SFAk_t-k_e model:

1. The percentage of additive genetic variance explained for individual trait by environment combinations is:

$$\mathbf{v} = 100\ \mathrm{diag}\left(\hat{\mathbf{\Lambda}}\hat{\mathbf{\Lambda}}^\top\right) \oslash \mathrm{diag}\left(\hat{\mathbf{\Lambda}}\hat{\mathbf{\Lambda}}^\top + \hat{\mathbf{\Psi}}_\mathbf{t} \otimes \mathbf{I}_p + \mathbf{I}_q \otimes \hat{\mathbf{\Psi}}_\mathbf{e}\right), \tag{21}$$

   where $\hat{\mathbf{\Lambda}} = [\hat{\mathbf{\Lambda}}_\mathbf{t} \otimes \hat{\mathbf{\Lambda}}_\mathbf{e}]$ and $\oslash$ is the Hadamard element-wise division operator. The overall percentage of variance explained across all traits and environments is $\bar{v} = \mathbf{1}_{ps}^\top \mathbf{v}/ps$.

2. The percentage of additive genetic variance explained for individual traits is:

$$\mathbf{v_t} = 100\ \mathrm{diag}\left(\hat{\mathbf{\Lambda}}_\mathbf{t}\hat{\mathbf{\Lambda}}_\mathbf{t}^\top \mathrm{tr}\left[\hat{\mathbf{\Lambda}}_\mathbf{e}\hat{\mathbf{\Lambda}}_\mathbf{e}^\top\right]/p\right) \oslash \bar{\mathbf{g}}_\mathbf{t}\ , \tag{22}$$

   where $\bar{\mathbf{g}}_\mathbf{t}$ is the s-vector of variances for individual traits defined in Equation 26. The percentage of variance explained across all traits is $\bar{v}_t = \mathbf{1}_s^\top \mathbf{v_t}/s$.

3. The percentage of additive genetic variance explained for individual environments is:

$$\mathbf{v_e} = 100\ \mathrm{diag}\left(\mathrm{tr}\left[\hat{\mathbf{\Lambda}}_\mathbf{t}\hat{\mathbf{\Lambda}}_\mathbf{t}^\top\right]\hat{\mathbf{\Lambda}}_\mathbf{e}\hat{\mathbf{\Lambda}}_\mathbf{e}^\top/s\right) \oslash \bar{\mathbf{g}}_\mathbf{e}\ , \tag{23}$$

   where $\bar{\mathbf{g}}_\mathbf{e}$ is the p-vector of variances for individual environments defined in Equation 26. The percentage of variance explained across all environments is $\bar{v}_e = \mathbf{1}_p^\top \mathbf{v_e}/p$.

The final model order is typically chosen such that $\bar{v}$, $\bar{v}_t$ and $\bar{v}_e$ are sufficiently high and the number of traits and environments with low variance explained in $\mathbf{v_t}$ and $\mathbf{v_e}$ is small. Similar measures can be obtained for the NFAk and UFAk_e models.

2.9 Genetic correlations between traits and environments

The additive genetic variance matrices between traits for environment j and between environments for trait i are given by:

$$\mathbf{G}_{\mathbf{t}_j} = \hat{\mathbf{\Lambda}}_\mathbf{t}\hat{\mathbf{\Lambda}}_\mathbf{t}^\top[\mathbf{\Lambda}_{\mathbf{e}_j}\mathbf{\Lambda}_{\mathbf{e}_j}^\top] + \hat{\mathbf{\Psi}}_\mathbf{t} + \hat{\psi}_{e_j}\mathbf{I}_s, \tag{24}$$

and

$$\mathbf{G}_{\mathbf{e}_i} = [\hat{\mathbf{\Lambda}}_{\mathbf{t}_i}\hat{\mathbf{\Lambda}}_{\mathbf{t}_i}^\top]\hat{\mathbf{\Lambda}}_\mathbf{e}\hat{\mathbf{\Lambda}}_\mathbf{e}^\top + \hat{\psi}_{t_i}\mathbf{I}_p + \hat{\mathbf{\Psi}}_\mathbf{e}, \tag{25}$$

which are $s \times s$ and $p \times p$ matrices, respectively, where $\hat{\mathbf{\Lambda}}_{\mathbf{e}_j}^\top = (\hat{\lambda}_{j;1}, \ldots, \hat{\lambda}_{j;k_e})^\top$ and $\hat{\mathbf{\Lambda}}_{\mathbf{t}_i}^\top = (\hat{\lambda}_{i;1}, \ldots, \hat{\lambda}_{i;k_t})^\top$.

The overall additive genetic variance matrices are given by:

$$\bar{\mathbf{G}}_\mathbf{t} = \sum_{j=1}^{p} \mathbf{G}_{\mathbf{t}_j}/p \qquad \text{and} \qquad \bar{\mathbf{G}}_\mathbf{e} = \sum_{i=1}^{s} \mathbf{G}_{\mathbf{e}_i}/s, \tag{26}$$

where $\bar{\mathbf{g}}_\mathbf{t} = \mathrm{diag}(\bar{\mathbf{G}}_\mathbf{t})$ and $\bar{\mathbf{g}}_\mathbf{e} = \mathrm{diag}(\bar{\mathbf{G}}_\mathbf{e})$ are the vectors in Equations 22 and 23, respectively. The variance matrices above are then converted to correlation matrices for interpretability (see Cullis et al., 2010). Similar correlation matrices can be obtained for the NFAk and UFAk_e models.

2.10 Selection tools

This section extends the selection tools of Smith and Cullis (2018) to the SFA-LMM. This extension requires rotation of the loadings and scores to a principal component solution, such that the rotated factors are orthogonal and sorted in decreasing order (see Cullis et al., 2010). A separate rotation is used for trait i, with:

$$\hat{\mathbf{\Lambda}}_i^* = c_i\hat{\mathbf{\Lambda}}_\mathbf{e}\mathbf{V_e} \qquad \text{and} \qquad \tilde{\mathbf{f}}_i^* = \left(\hat{\mathbf{\Lambda}}_{\mathbf{t}_i} \otimes \mathbf{V}_\mathbf{e}^\top \otimes \mathbf{I}_v\right)\tilde{\mathbf{f}}_\mathbf{te}/c_i, \tag{27}$$

where $c_i = \pm\sqrt{\hat{\mathbf{\Lambda}}_{\mathbf{t}_i}\hat{\mathbf{\Lambda}}_{\mathbf{t}_i}^\top}$ and $\mathbf{\Lambda}_{\mathbf{t}_i}$ is defined in Equation 25. The sign of c_i is chosen as either -1 or 1 to ensure the correlations between traits are preserved within the loadings. The $k_e \times k_e$ rotation matrix $\mathbf{V_e}$ is obtained via the singular value decomposition $\hat{\mathbf{\Lambda}}_\mathbf{e} = \mathbf{U_e}\mathbf{D}_\mathbf{e}^{1/2}\mathbf{V}_\mathbf{e}^\top$.

Overall performance and stability

The overall performance vector for trait i is given by:

$$\mathrm{OP}_i = (\bar{\boldsymbol{\lambda}}^*_{i;1} \otimes \mathbf{I}_v)\tilde{\mathbf{f}}^*_{i;1}, \tag{28}$$

where $\bar{\boldsymbol{\lambda}}^*_{i;1} = \mathbf{1}_p^\top\hat{\boldsymbol{\lambda}}^*_{i;1}/p$ is the estimated mean loading for the first rotated factor and $\tilde{\mathbf{f}}^*_{i;1}$ is the corresponding v-vector of predicted scores. OP_i can therefore be viewed as the expected genotype performance for the i^{th} trait in an average (typical) environment.

The stability vector for trait i is given by:

$$\mathrm{RMSD}_i = \sqrt{\mathrm{diag}(\tilde{\mathbf{E}}_i^\top\tilde{\mathbf{E}}_i)/p}, \tag{29}$$

where $\tilde{\mathbf{E}}_i = \tilde{\mathbf{F}}^*_i\hat{\mathbf{\Lambda}}^{*\top}_i - \tilde{\mathbf{f}}^*_{i;1}\hat{\boldsymbol{\lambda}}^{*\top}_{i;1}$ is a $v \times p$ matrix of additive GET effects associated with rotated factors $l_e \geq 2$ and $\tilde{\mathbf{F}}^*_i = [\tilde{\mathbf{f}}^*_{i;1}\ \tilde{\mathbf{f}}^*_{i;2}\ \ldots\ \tilde{\mathbf{f}}^*_{i;k_e}]$ is a $v \times k_e$ matrix of predicted genotype scores. RMSD_i can therefore be viewed as the variance in genotype performance across all environments.

The measures of OP_i and RMSD_i can be used for selection, and can be visualised using latent regression plots or scatter plots. The latent regression plots used in this paper are an extension of Cullis et al. (2014), while the scatter plots are an extension of Smith and Cullis (2018). Lastly, OP_i and RMSD_i can be supplemented with two measures of variance explained for trait i:

1. The percentage of additive genetic variance explained by individual rotated factors is:

$$\mathbf{v}_i = 100\ \mathrm{diag}\left(\hat{\mathbf{\Lambda}}^{*\top}_i\hat{\mathbf{\Lambda}}^*_i\right)\Big/\mathrm{tr}\left(\bar{\mathbf{G}}_{\mathbf{e}_i}\right), \tag{30}$$

   where $\bar{\mathbf{G}}_{\mathbf{e}_i}$ is defined in Equation 26. The measure in Equation 22 for the i^{th} trait is then given by $v_{t_i} = \mathbf{1}^\top_{k_e}\mathbf{v}_i$.
2. The percentage of additive genetic variance explained within individual environments is:

$$\mathbf{v}_{\mathbf{e}_i} = 100\ \mathrm{diag}\left(\hat{\mathbf{\Lambda}}^*_i\hat{\mathbf{\Lambda}}^{*\top}_i\right) \oslash \bar{\mathbf{g}}_{\mathbf{e}_i}, \tag{31}$$

where $\bar{\mathbf{g}}_{\mathbf{e}_i} = \mathrm{diag}\left(\bar{\mathbf{G}}_{\mathbf{e}_i}\right)$.

Selection index

The separate OP_i and RMSD_i measures can be combined across traits to form a selection index. The selection index for overall performance is given by:

$$\begin{aligned}\mathcal{I} &= \omega_1\bar{\mathrm{OP}}_1 + \omega_2\bar{\mathrm{OP}}_2 + \ldots + \omega_s\bar{\mathrm{OP}}_s \\ &= (\boldsymbol{\omega}^\top \otimes \mathbf{I}_v)\,\bar{\mathrm{OP}}\end{aligned} \tag{32}$$

where $\boldsymbol{\omega} = (\omega_1, \omega_2, \ldots, \omega_s)^\top$ is an s-vector of user supplied weights for each trait and $\bar{\mathrm{OP}} = (\bar{\mathrm{OP}}_1^\top, \bar{\mathrm{OP}}_2^\top, \ldots, \bar{\mathrm{OP}}_s^\top)^\top$ is a vs-vector of standardised overall performances in which $\bar{\mathrm{OP}}_i = \tilde{\mathbf{f}}^*_{i;1}$ is the v-vector for the i^{th} trait.

The selection index can be supplemented with a measure of (model-based) accuracy for each genotype, with:

$$\mathrm{acc}(\mathcal{I}) = \sqrt{\mathbf{1}_{vs} - \mathrm{diag}\left[\mathrm{PEV}(\mathcal{I}) \oslash \mathrm{var}(\mathcal{I})\right]}. \tag{33}$$

The prediction error variance matrix is given by:

$$\mathrm{PEV}(\mathcal{I}) = \left(\mathbf{\Omega}^\top \otimes \mathbf{v}^\top_{\mathbf{e}_1} \otimes \mathbf{I}_v\right)\mathrm{PEV}\left(\tilde{\mathbf{f}}\right)\left(\mathbf{\Omega} \otimes \mathbf{v}_{\mathbf{e}_1} \otimes \mathbf{I}_v\right) \tag{34}$$

where $\mathbf{\Omega} = \mathbf{\Lambda}^\top_\mathbf{t}\mathbf{C}^{-1}\boldsymbol{\omega}$, with $\mathbf{C} = \oplus^s_{i=1}c_i$, $\mathbf{v}_{\mathbf{e}_1}$ is the first column of $\mathbf{V_e}$ in Equation 27 and $\mathrm{PEV}(\tilde{\mathbf{f}})$ is the prediction error variance matrix of $\tilde{\mathbf{f}}$.

The variance matrix is given by:

$$\mathrm{var}(\mathcal{I}) = \mathbf{\Omega}^\top\mathbf{\Omega} \otimes \mathbf{G_g}. \tag{35}$$

Note that accuracies for the separate OP_i measures can be obtained using a similar approach. These accuracies will be particularly useful for incomplete multi-trait MET datasets where some traits are measured in some environments but not others.

3 Results

This section presents the results from fitting the separable and non-separable linear mixed models to the multi-trait MET dataset. The dataset comprises 262 test genotypes and four check cultivars that were evaluated for three agronomic traits (YLD, DTF, and PHT) across 12 environments in the south-eastern rice growing region of Australia. The important results from each model are detailed below, along with application of the selection tools to the Australian Rice Breeding Program.

3.1 Baseline diagonal model

The analyses began by fitting a non-separable diagonal model, which assumes the additive GET effects for each trait by environment combination are independent (Table 3). This process resembles initial single-trait single-environment analyses that should be performed on multi-trait MET datasets before more complex models are considered. These analyses are used to examine genetic and non-genetic sources of variation, identify potential outliers and address spatial variations (see the Supplementary Material).

The non-separable diagonal model was also used to compare the two residual spatial models, that is *diag** and *diag* in Table 3. The two spatial models have very similar AIC (-6519.0 compared to -6515.1), but have different numbers of residual parameters (108 compared to 55). This indicates that the spatial model in *diag* provides a comparably good fit with fewer parameters, and was thence used in all subsequent analyses.

3.2 Non-separable factor analytic linear mixed model (NFA-LMM)

The analyses then proceeded by fitting a series of NFA-LMMs (Table 3). The distinguishing feature of the NFA-LMM is that the additive GET effects for different trait by environment combinations are now assumed to be correlated. These models provide a much better fit to the multi-trait MET dataset compared to the baseline diagonal models. The final order was selected using the formal and informal measures similar to those in Section 2.8. Only $k = 3$ factors were required to achieve an adequate fit and sufficient percentage of additive genetic variance explained across traits ($\bar{v}_t = 86.2\%$), environments ($\bar{v}_e = 86.8\%$) and overall ($\bar{v} = 87.1\%$). The latter measure reflects the percentage of GETI common to multiple (at least two) trait by environment combinations. The remaining 12.9% not explained by the common factors then reflects residual GETI specific to individual trait by environment combinations. Higher order models were fitted, but proved unnecessarily complicated (Table 3).

3.3 Unstructured factor analytic linear mixed model (UFA-LMM)

The analyses then proceeded by fitting a series of UFA-LMMs (Table 4a). The distinguishing feature of the UFA-LMM is that it has a separable model between traits and environments, and thence has much fewer variance parameters than the NFA-LMM. Only $k_e = 2$ environmental factors were required to achieve an adequate fit and sufficient percentage of additive genetic variance explained across traits ($\bar{v}_t = 83.3\%$), environments ($\bar{v}_e = 78.1\%$) and overall ($\bar{v} = 81.5\%$). The latter measure reflects the percentage of GETI common to multiple environments. The remaining 18.5.4% not explained by the environmental factors reflects residual GETI specific to individual traits.

3.4 Partially separable factor analytic linear mixed model (SFA-LMM)

The analyses concluded by fitting a series of SFA-LMMs (Table 4b). The distinguishing feature of the SFA-LMM is that it includes a partially separable factor analytic model between traits and between environments. The SFA-LMM therefore has much fewer variance parameters than the NFA-LMM, and will have much fewer parameters than the UFA-LMM as the number of traits increases. Only $k_t = 3$ and $k_e = 2$ factors were required to reach an adequate fit and sufficient percentage of additive genetic variance explained across traits ($\bar{v}_t = 76.2\%$), environments ($\bar{v}_e = 77.5\%$) and overall ($\bar{v} = 80.8\%$). The latter measure reflects the percentage of GETI common to multiple traits and multiple environments. The remaining 18.9% not explained by the trait and environmental factors reflects residual GETI specific to individual traits and/or environments.

3.5 Model comparison

Formal model selection criteria was used to compare the selected SFA3-2 and UFA2 models (Table 4). The SFA3-2 model has more additive genetic variance parameters (42 compared to 31), but has a much lower AIC (-6,982.0 compared to -6970.9). This indicates that the SFA3-2 model provides a superior fit than the UFA2 model with three traits, and suggests that it will provide a superior fit with fewer variance parameters as the number of traits increases. The NFA3 model does have a better AIC than the SFA3-2 model, however, note that it estimates ~ 3.5 times more additive genetic variance parameters with only three traits and 12 environments (141 compared to 42). This difference will become even more apparent for a larger number of traits and environments.

3.6 Model summaries

Table 5 presents a summary of the three agronomic traits and 12 rice growing environments for the SFA3-2 model. Note that these summaries correspond to the scaled phenotypes. The additive genetic variance for traits, $\bar{\mathbf{g}}_\mathbf{t}$, was 0.36 for YLD, 3.03 for DTF and 16.06 for PHT . The additive genetic variance for environments, $\bar{\mathbf{g}}_\mathbf{e}$, was highest for 18MB_E (14.25) and lowest for 17MB_L (2.43). By design, the overall variance across traits and environments is the same, and equal to $\bar{g} = 6.48$. The percentage of variance explained for traits, $\mathbf{v_t}$, was highest for PHT (95.3%) and then DTF (73.7%), but note that only 60.0% was explained for YLD. The percentage of variance explained for environments, $\mathbf{v_e}$, was highest for 17MB_E (92.3%) while all other environments were >60% explained except for 17MV_E (48.4%). Lastly, Table 5 presents the REML estimates of the unrotated factor loadings. These matrices demonstrate the structure of $\mathbf{G}$, and the constraints required during estimation (Section 2.7).

Genetic correlations between traits and environments

Table 6 presents the REML estimates of the additive genetic correlations between traits for each environment, while Figure 3 presents the additive genetic correlations between environments for each trait. These matrices are used to examine GETI from the perspective of the traits and the environments.

Table 6 shows that the additive genetic correlations between traits are different for each environment. These correlations were obtained from $\bar{\mathbf{G}}_{\mathbf{t}_j}$ in Equation 24. The correlations between YLD and DTF were almost zero for all environments, with -0.02 overall. In terms

of YLD and PHT, the correlations were highest for $17MV_E$ (-0.23) and lowest for $17MB_E$ (-0.42) with -0.36 overall. In terms of DTF and PHT, the correlations were highest for $17MV_E$ (-0.09) and lowest for six environments (-0.23), with -0.20 overall. This indicates substantial dissimilarity in genotype rankings between YLD and DTF, and a reversal of rankings between PHT and each of these traits.

The heatmaps in Figure 3 show that the additive genetic correlations between environments are different for each trait. These correlations were obtained from $\bar{\mathbf{G}}_{\mathbf{e}_i}$ in Equation 25 and ordered based on a dendrogram applied to YLD (see Cullis et al., 2010). There are three important features of the heatmaps:

1. The GEI patterns are substantially different for each trait, especially YLD. The correlations for YLD range from 0.30 to 0.70 (mean of 0.52), for DTF they range from 0.26 to 1.00 (mean of 0.73) and for PHT they range from 0.66 to 0.98 (mean of 0.88). This indicates considerable dissimilarity in genotype rankings between environments for YLD and thence considerable crossover GEI. The opposite is true for DTF (except $17MV_E$ and $18MB_M$) and PHT.
2. There is little structure to the overall GEI patterns across traits, that is GEI is not aligned with year, region or season.
3. The lowest correlations correspond to $17MV_E$ and $18MB_M$, especially for YLD and DTF. These two environments also have the lowest variance explained (Table 5).

Table 6 and Figure 2 provide summaries of GETI from the perspective of the traits and environments. The selection tools demonstrated below enable GETI to be summarised from the perspective of the genotypes.

3.7 Selection tools

The selection tools were applied to the SFA3-2 model in terms of the additive GET effects. These tools provide breeders with measures of overall performance (OP_i) and stability ($RMSD_i$) for each trait. Selection will be demonstrated separately for each trait and then together using a selection index.

Overall performance and stability

Table 7 presents the REML estimates of the rotated factor loadings for each trait, while Figure 4 presents latent regression plots and OP_i vs $RMSD_i$ plots for each genotype. This information is used to demonstrate selection within each trait. YLD is the primary trait of economic importance, and thence the focus in the following.

The OP_i measure for YLD is a function of the first rotated factor, which explains $v_{1;1} = 57.3\%$ of the additive genetic variance (Table 7a). Since all loadings for this factor are positive, the fitted GET effects capture non-crossover GEI only (see Smith and Cullis, 2018). This feature can be visualized using the latent regression plot in Figure 4a for reference genotypes G1-G4, where the regression lines diverge and never crossover. OP_i is therefore given by the fitted GET effect at the mean loading of 0.44 (*vertical dotted line*), that is 0.96 for G1, 0.37 for G2, -0.40 for G3 and -1.79 t/ha for G4. This measure reflects the expected YLD performance for G1-G4 in an average environment.

The $RMSD_i$ measure for YLD is a function of the second rotated factor, which only explains $v_{1;2} = 3.7\%$ of the additive genetic variance (Table 7a). Since this factor comprises both positive and negative loadings, the regression lines crossover (not shown) and the fitted GET effects predominately capture crossover GEI only. The $RMSD_i$ measure can also be visualised using the latent regression plot in Figure 4a. $RMSD_i$ is equal to the root mean square of the deviations around the first factor regression line, that is 0.03 for G1, 0.01 for G2, 0.02 for G3 and 0.14 for G4 t/ha. This measure reflects the variance in YLD performance across environments for G1-G4.

Selection across all genotypes for YLD can then be achieved using the OP vs RMSD plot in Figure 4a. Consistently high performing (yielding) genotypes occur at the top left of this figure. For example, G1 is high yielding and stable since it has high OP and low RMSD. By comparison, poor yielding and unstable genotypes which have low OP and high RMSD occur at the bottom right (see, for example, G4). The remaining highlighted genotypes are high (G2, Kyeema and Langi), average (Topaz) or low (G3) yielding but stable. Similar interpretation can be made for DTF and PHT in Figures 4a and b, but note that the first rotated factor explains 69.5 and 90.5 % of the additive genetic variance in these traits (Tables 7b and c). Also note that genotypes of high interest occur at the bottom left for these traits, such as G3 which flowers consistently early and G2 which grows consistently short.

Selection Index

Figure 5 presents a parallel coordinate plot with standardised OP for each trait, as well as a selection index. The weights used in this index were 0.7, -0.2 and -0.1 for YLD, DTF and PHT, respectively. Note that the weights are arbitrary and are used to illustrate the concepts and methods developed in Section 2. The extension to economic weights is straightforward. The selection index is used to achieve simultaneous selection across all traits. For example, G1 is higher yielding and has a similar flowering time to G2, however, they have the same index value since G2 is much shorter than G1. Both genotypes also have a higher index than the four check culitvars and G3. By comparison, G4 is much lower yielding and much taller than all other test genotypes, and thence has a much lower index value. Lastly,

note that the patterns observed in the standardised OP measures for YLD, DTF and PHT reflect the observed variances for these traits (Table 5), as well as the observed correlations between traits (Table 6).

4 Discussion

This paper developed a single-stage GS approach which incorporates information on multiple traits and multiple environments within a partially separable factor analytic framework. The factor analytic linear mixed model of Smith et al. (2001) is an effective method for analysing MET datasets, but is yet to be extended to GS for multiple traits and multiple environments. The advantage of incorporating both sources of information is that breeders can utilise GETI to obtain more accurate predictions of the GET effects across both factors. The partially separable factor analytic linear mixed model (SFA-LMM) developed in this paper is based on a three-way separable structure, with a factor analytic model for traits, a factor analytic model for environments and a genomic relationship matrix for genotypes. This approach is a natural extension of the factor analytic linear mixed model, which has been widely adopted in most major Australian plant breeding programs (Smith et al., 2015).

Plant breeders select superior genotypes with regards to performance across a set of production environments for multiple traits of commercial importance. Plant breeding datasets are therefore naturally generated as *multi-trait* MET datasets. Many of the current statistical approaches, however, only include models for GEI within single traits or models for GTI within single environments, but very few have considered appropriate models for GETI across multiple traits and environments. Recently, Montesinos-López et al. (2018) demonstrated a restrictive model for GETI which assumes the same GEI pattern for each trait and the same GTI pattern for each environment. They also did not address spatial variation and other non-genetic sources (also see Montesinos-López et al., 2016b; Volpato et al., 2019).

The approach of Smith et al. (2019) includes a less restrictive model for GETI and accommodates non-genetic sources of variation. Their approach includes an unstructured variance matrix for traits (treatments) and a factor analytic variance matrix for environments, but they only consider a diagonal matrix for genotypes. There are two limitations of their approach: i) the unstructured matrix becomes computationally prohibitive for a large number of traits and ii) they do not consider GS. Meyer (2009) did previously suggest that a separable factor analytic model could be used for traits as well as environments, but this was never put into practice. The SFA-LMM developed in this paper extends the approach of Smith et al. (2019) for GS using a partially separable factor analytic model across multiple traits and multiple environments.

There are three appealing features of the SFA-LMM which address the limitations of current statistical approaches:

1. *Dimension reduction:* The SFA-LMM includes a partially separable factor analytic model for GETI in terms of a small number of trait and environmental factors. This enables common information to be shared across both factors while simultaneously reducing their dimension.
2. *Interpretability:* The SFA-LMM captures a different GTI pattern for each environment and a different GEI pattern for each trait. This provides an appropriate framework to summarise GETI in multi-trait MET datasets.
3. *Efficient selection:* The SFA-LMM provides a natural framework for applying plant breeding selection tools. This enables breeders to obtain measures of OP_i and RMSD_i for each trait as well as an overall selection index.

The SFA-LMM was demonstrated on a multi-trait MET dataset from The Australian Rice Breeding Program. The dataset comprises 262 test genotypes and four check cultivars that were evaluated for three agronomic traits across 12 environments in the south-eastern rice growing region of Australia. This dataset was used to illustrate the concepts and methods developed in Section 2. Note, however, it only includes a very small number of traits and therefore does not exploit the potential of the SFA-LMM to analyse a large number of traits. The practical implication of this will be discussed further below.

There are three important results from fitting the SFA-LMM which highlight its practicality for analysing multi-trait MET datasets:

1. The selected SFA3-2 model provides a better fit than the UFA2 model in terms of AIC, and is more parsimonious than the NFA3 model (Tables 3 and 4). The SFA model will also be more parsimonious than the UFA model when the number of traits increases. This highlights the advantage modelling GETI in terms of a small number of trait and environmental factors.
2. The additive genetic correlations between traits are higher for 17MV_E and 18MB_M compared to all other environments (Table 6). The correlations between environments are much higher for DTF and PHT compared to YLD (Figure 3). This highlights the ability of the SFA-LMM to capture a different GTI pattern for each environment and a different GEI pattern for each trait.
3. The selection index was demonstrated for 262 test genotypes and four check cultivars in the multi-trait MET dataset. This index enables breeders to make efficient selections for multiple traits based on genotype performance across multiple environments.

Each point will now be discussed further.

With regards to point 1, Meyer (2009) warned about the challenges of using factor analytic models when the covariances between traits cannot be attributed to a small number of common factors. This is often the case when the correlations between traits are low and/or the number of traits is small, which restricts the maximum number of factors that can be fitted. This issue was observed for the current multi-trait MET dataset which only includes three traits. The additive genetic variance explained for YLD was only 60.4% and this will likely increase with additional (correlated) traits. The application of the SFA-LMM to a larger multi-trait MET dataset with more traits is the topic of current research.

With regards to point 2, understanding the genetic correlations between environments provides valuable information for making selection decisions. The correlations for YLD show no clear year, location or seasonal pattern (Figure 3). This is consistent with the complex nature of GEI in the south-eastern Australian rice growing region, which is driven by complex environmental factors such as reproductive cold damage from infrequent cool weather periods during microspore development (Williams and Angus, 1994). By comparison, the correlations between environments for DTF and PHT are high, which reflects their generally high line-mean heritability in the breeding program and in rice germplasm more broadly (Wei et al., 2020). This also demonstrates that there is little crossover GEI in these traits. The only exceptions are $17MV_E$ and $18MB_M$ for DTF which are not well correlated with the remaining environments. The trials in these environments may have experienced different management practices or extreme growing conditions. Regardless, the SFA-LMM has a natural way of accommodating such environments, where their low variance explained also reflects their low contribution to the model.

Understanding the genetic correlation between traits also provides valuable information for making selection decisions. The lack of correlation between YLD and DTF (-0.02) indicates that the current breeding germplasm could be subject to selection for DTF without impacting YLD. For example, there is a need to develop high yielding cultivars for both short season (early flowering time) and full season (late flowering time), and the low correlation suggests that both breeding targets could be pursued with the current germplasm. The negative correlation between YLD and PHT (-0.36) indicates that shorter genotypes tend to be higher yielding. This could be due to the interaction between lodging and yield. Generally, taller genotypes in the south-eastern growing region are more prone to lodging at maturity (Lewin and Heenan, 1987). This makes harvest more difficult and results in lower yields (Ookawa et al., 2010). Harvest index (grain yield as a fraction of total above ground biomass) may also explain the negative correlation between YLD and PHT. Breeding programs across a range of cereals have manipulated harvest index to increase yields, most notably through indirect selection for the semi-dwarfing trait since this is easier than selecting for biomass directly (Hay, 1995; Sinclair, 1998). Lastly, the negative correlation between DTF and PHT (-0.20) indicates that taller genotypes tend to flower early. This correlation may be a result of the breeding objectives where selection is primarily for high yielding and short genotypes, and secondarily for early flowering genotypes. The observed correlation between DTF and PHT could be an indirect result of this selection strategy.

With regards to point 3, rice breeders select genotypes that are high yielding, early flowering and short. These selections can be made using the OP vs RMSD plots in Figure 4 for each trait separately. For example, genotype G1 would be selected for YLD, G3 would be selected for DTF and G2 would be selected for PHT. This approach is similar to traditional threshold selection, with the exception that genotypes are now selected based on their overall performance as well as their stability (Smith and Cullis, 2018). With more than one trait, however, this approach is inefficient and ignores the genetic correlations between traits. The selection index in Figure 5 weights the importance of individual traits based on the breeding objectives. This index utilises the common information across the traits and environments within the SFA-LMM, and thence enables breeders to make efficient selections across multiple traits. Note that the selection index demonstrated in this paper was based on OP alone since the variance explained by the higher order factors is very small. The importance of RMSD will likely increase as the number of traits increases.

The selection index provides important information on the overall merit of test genotypes compared to the check cultivars. The check cultivars provide a baseline for the three traits under selection. For example, Langi is a high yielding and soft cooking long grain cultivar which is broadly adapted across the Australian rice growing area. Doongara is a semi-dwarf japonica long grain variety that flowers late and can be high yielding under favourable conditions, being susceptible to reproductive cold damage at all growth stages. Kyeema is a tall jasmine style cultivar that does not have the semi-dwarf trait. Kyeema was superseded by Topaz, which is a semi-dwarf jasmine style cultivar with notably later flowering time than the other three check cultivars. The selection index highlights numerous test genotypes which have a higher overall merit than the check cultivars (e.g. G1 and G2). This demonstrates the immediate genetic gain that can be made in the Australian rice breeding program. The parallel coordinate plot in Figure 5 also highlights numerous test genotypes that should be retained in the programme as parents to maintain genetic variation in the traits under selection, although they may not be candidates for release. For example, G1 is a high-yielding and early flowering genotype which may be too tall for commercial release.

The inclusion of multiple traits and multiple environments within a single-stage SFA-LMM provides breeders with an informative framework to utilise GETI for GS. This approach represents an important continuation in the advancement of statistical analyses of plant breeding datasets, particularly with the advent of high throughput phenotypic data involving a very large number of traits and environments. It also represents an appropriate approach to handle incomplete data where some traits are measured in some environments but not others.

Data Availability

The data that support the findings of this study are available on on the New South Wales Government data repository (https://data.nsw.gov.au).

Code Availability

The `R` scripts to perform the analyses using `ASReml-R` are available on the GitHub repository (https://github.com/HighlanderLab/jbancic_mtme_fa).

Acknowledgements

JB thanks Scotland's Rural College (SRUC) for funding his PhD studentship Research Excellence Grant. GG acknowledges funding from the BBSRC Strategic Programme to The Roslin Institute (BBS/E/D/30002275) and the University of Edinburgh's Data-Driven Innovation Chancellor's fellowship. Lastly, The Australian Rice Breeding Program is funded under the Australian Rice Partnership II project, a partnership between NSW Department of Primary Industries, AgriFutures and SunRice.

Author Contributions

DT conceived and developed the methodology. DT and JB curated the data, conducted the analyses and wrote the manuscript. BO curated the data and wrote the plant breeding perspectives. GG reviewed the manuscript and provided quantitative genetics perspectives. All authors have read and approved the manuscript.

Conflict of Interest

The authors declare that they have no conflict of interest.

References

Bailey RA (2008) Design of Comparative Experiments. Cambridge University Press, Cambridge

Bernardo R (2010) Breeding for Quantitative Traits in Plants, 2nd edn. Stemma Press, Woodsbury, MN

Butler D (2019) pedicure: pedigree tools. URL https://mmade.org/pedicure/

Butler DG, Cullis BR, Gilmour AR, Gogel BJ, Thompson R (2017) ASReml-R Reference Manual Version 4. ASReml-R Reference Manual p 176, URL http://www.homepages.ed.ac.uk/iwhite/asreml/uop.

Cullis BR, Smith AB, Beeck CP, Cowling WA (2010) Analysis of yield and oil from a series of canola breeding trials, part II: Exploring variety by environment interaction using factor analysis. Genome 53:1002–1016, URL http://doi.org/10.1139/G10-080

Cullis BR, Jefferson P, Thompson R, Smith AB (2014) Factor analytic and reduced animal models for the investigation of additive genotype by environment interaction in outcrossing plant species with application to a *p*inus radiata breeding program. Theoretical and Applied Genetics 127:2193–2210, URL http://doi.org/10.1007/s00122-014-2373-0

Faveri JD, Verbyla AP, Cullis BR, Pitchford WS, Thompson R (2017) Residual Variance-Covariance Modelling in Analysis of Multivariate Data from Variety Selection Trials. Journal of Agricultural, Biological, and Environmental Statistics 22(1):1–22, DOI 10.1007/sl3253-016-0267-0

Gilmour AR, Thompson R, Cullis BR (1995) Average information reml: An efficient algorithm for variance parameter estimation in linear mixed models. Biometrics 51(4):1440–1450, URL http://www.jstor.org/stable/2533274

Gilmour AR, Cullis BR, Verbyla AP (1997) Accounting for natural and extraneous variation in the analysis of field experiments. Journal of Agricultural, Biological, and Environmental Statistics 2:269–293, URL http://doi.org/10.2307/1400446

Hay RK (1995) Harvest index: a review of its use in plant breeding and crop physiology. Annals of Applied Biology 126(1):197–216, DOI 10.1111/j.1744-7348.1995.tb05015.x

Lewin L, Heenan D (1987) The Agronomy of Rice Production in the Riverina Region of Southeastern Austialia. In: Efficiency of nitrogen fertilizers for rice: proceedings of the Meeting of the International Network on Soil Fertility and Fertilizer Evaluation for Rice, Griffith, New South Wales, Australia, pp 69–80

Meuwissen THE, Hayes BJ, Goddard ME (2001) Prediction of Total Genetic Value Using Genome-Wide Dense Marker Maps. Genetics 157:1819–1829, URL http://doi.org/10.1017/S0021859600043392

Meyer K (2007) Multivariate analyses of carcass traits for Angus cattle fitting reduced rank and factor analytic models. Journal of Animal Breeding and Genetics 124(2):50–64, DOI 10.1111/j.1439-0388.2007.00637.x

Meyer K (2009) Factor-analytic models for genotype × environment type problems and structured covariance matrices. Genetics Selection Evolution 41(1):1–11, DOI 10.1186/1297-9686-41-21

Michel S, Löschenberger F, Ametz C, Pachler B, Sparry E, Bürstmayr H (2019) Simultaneous selection for grain yield and protein content in genomics-assisted wheat breeding. Theoretical and Applied Genetics 132(6):1745–1760, DOI 10.1007/s00122-019-03312-5, URL https://doi.org/10.1007/s00122-019-03312-5

Montesinos-López OA, Montesinos-López A, Crossa J, Toledo FH, Pérez-Hernández O, Eskridge KM, Rutkoski J (2016a) A genomic bayesian multi-trait and multi-environment model. G3: Genes, Genomes, Genetics 6(9):2725–2774, DOI 10.1534/g3.116.032359

Montesinos-López OA, Montesinos-López A, Crossa J, Toledo FH, Pérez-Hernández O, Eskridge KM, Rutkoski J (2016b) A genomic bayesian multi-trait and multi-environment model. G3: Genes, Genomes, Genetics 6(9):2725–2774, DOI 10.1534/g3.116.032359

Montesinos-López OA, Montesinos-López A, Crossa J, Gianola D, Hernández-Suárez CM, Martín-Vallejo J (2018) Multi-trait, multi-environment deep learning modeling for genomic-enabled prediction of plant traits. G3: Genes, Genomes, Genetics 8(12):3829–3840, DOI 10.1534/g3.118.200728

Montesinos-López OA, Montesinos-López A, Hernández MV, Ortiz-Monasterio I, Pérez-Rodríguez P, Burgueño J, Crossa J (2019) Multivariate bayesian analysis of on-farm trials with multiple-trait and multiple-environment data. Agronomy Journal 111(6):2658–2669, DOI 10.2134/agronj2018.06.0362

Oakey H, Verbyla AP, Pitchford W, Cullis BR, Kuchel H (2006) Joint modeling of additive and non-additive genetic line effects in single field trials. Theoretical and Applied Genetics 113:809–819, URL http://doi.org/10.1007/s00122-006-0333-z

Oakey H, Verbyla AP, Cullis BR, Wei X, Pitchford WS (2007) Joint modelling of additive and non-additive (genetic line) effects in multi-environment trials. Theoretical and Applied Genetics 114:1319–1332, URL http://doi.org/10.1007/s00122-007-0515-3

Ookawa T, Hobo T, Yano M, Murata K, Ando T, Miura H, Asano K, Ochiai Y, Ikeda M, Nishitani R, Ebitani T, Ozaki H, Angeles ER, Hirasawa T, Matsuoka M (2010) New approach for rice improvement using a pleiotropic QTL gene for lodging resistance and yield. Nature Communications 1(8), DOI 10.1038/ncomms1132

R Core Team (2021) R: A Language and Environment for Statistical Computing. R: A Language and Environment for Statistical Computing, Vienna, Austria, URL https://www.r-project.org/

Sansaloni C, Petroli C, Jaccoud D, Carling J, Detering F, Grattapaglia D, Kilian A (2011) Diversity Arrays Technology (DArT) and next-generation sequencing combined: genome-wide, high throughput, highly informative genotyping for molecular breeding of Eucalyptus. BMC Proceedings 5(S7), DOI 10.1186/1753-6561-5-s7-p54

Sinclair TR (1998) Historical changes in harvest index and crop nitrogen accumulation. Crop Science 38(3):638–643, DOI 10.2135/cropsci1998.0011183X003800030002x

Slavov GT, Davey CL, Bosch M, Robson PR, Donnison IS, Mackay IJ (2019) Genomic index selection provides a pragmatic framework for setting and refining multi-objective breeding targets in Miscanthus. Annals of Botany 124(4):521–529, DOI 10.1093/aob/mcy187

Smith A, Borg L, Gogel B, Cullis B (2019) Estimation of factor analytic mixed models for the analysis of multi-treatment multi-environment trial data. Journal of Agricultural, Biological, and Environmental Statistics

Smith AB, Cullis BR (2018) Plant breeding selection tools built on factor analytic mixed models for multi-environment trial data. Euphytica 214:143–161, URL http://doi.org/10.1007/s10681-018-2220-5

Smith AB, Cullis BR, Thompson R (2001) Analyzing variety by environment data using multiplicative mixed models and adjustments for spatial field trend. Biometrics 57:1138–1147, URL http://doi.org/10.1111/j.0006-341X.2001.01138.x

Smith AB, Stringer JK, Wei X, Cullis BR (2007) Varietal selection for perennial crops where data relate to multiple harvests from a series of field trials. Euphytica 157(1-2):253–266, DOI 10.1007/s10681-007-9418-2

Smith AB, Ganesalingam A, Kuchel H, Cullis BR (2015) Factor analytic mixed models for the provision of grower information from national crop variety testing programs. Theoretical and Applied Genetics 128:55–72, URL http://doi.org/10.1007/s00122-014-2412-x

Stranden I, Garrick A (2009) Derivation of equivalent computing algorithms for genomic predictions and reliabilities of animal merit. Journal of Dairy Science 92:2971–2975, URL http://doi.org/10.3168/jds.2008-1929

Tolhurst DJ, Mathews KL, Smith AB, Cullis BR (2019) Genomic selection in multi-environment plant breeding trials using a factor analytic linear mixed model. Journal of Animal Breeding and Genetics 136:279–300, URL http://doi.org/10.1111/jbg.12404

Troyanskaya O, Cantor M, Sherlock G, Brown P, Hastie T, Tibshirani R, Botstein D, Altman RB (2001) Missing value estimation methods for DNA microarrays. Bioinformatics 17:520–525, URL http://doi.org/10.1093/bioinformatics/17.6.520

Ukrainetz NK, Yanchuk AD, Mansfield S (2018) Climatic drivers of genotype-environment interactions in lodgepole pine based on multi-environment trial data and a factor analytic model of additive covariance. Canadian Journal of Forest Research 48:835–854, URL http://doi.org/10.1139/cjfr-2017-0367

VanRaden PM (2008) Efficient Methods to Compute Genomic Predictions. Journal of Dairy Science 91:4414–4423, URL http://doi.org/10.3168/jds.2007-0980

Volpato L, Alves RS, Teodoro PE, De Resende MDV, Nascimento M, Nascimento ACC, Ludke WH, da Silva FL, Borém A (2019) Multi-trait multi-environment models in the genetic selection of segregating soybean progeny. PLoS ONE 14(4):1–22, DOI 10.1371/journal.pone.0215315

Wei J, Xie W, Li R, Wang S, Qu H, Ma R, Zhou X, Jia Z (2020) Analysis of trait heritability in functionally partitioned rice genomes. Heredity 124(3):485–498, DOI 10.1038/s41437-019-0244-9, URL http://dx.doi.org/10.1038/s41437-019-0244-9

Williams R, Angus J (1994) Deep floodwater protects high-nitrogen rice crops from low-temperature damage. Australian Journal of Experimental Agriculture 34(7):927 – 932, URL https://doi.org/10.1071/EA9940927

Table 1: The multi-trait MET dataset, Part 1: Summary of growing environments. Presented is the number of genotypes (with two, three or four replicates) and total number of plots. Also presented for grain yield (YLD), days to flowering (DTF) and plant height (PHT) is the mean, number of missing plots and generalised narrow-sense heritability (h^2). The data are presented such that the *white* and *grey blocks* represent the △ Murrumbidgee and × Murray Valley growing regions, respectively.

		Genotypes				Plots	YLD (t/ha)			DTF (days)			PHT (cm)		
Region	Env	Total	2rep	3rep	4rep	Total	Mean	NAs	h^2	Mean	NAs	h^2	Mean	NAs	h^2
	$17MB_E$	72	24	0	48	240	8.6	2	0.73	98.3	8	0.61	80.5	1	0.81
	$17MB_M$	60	0	0	60	240	8.5	5	0.64	91.7	0	0.51	80.3	0	0.66
	$17MB_L$	60	0	0	60	240	6.7	4	0.08	83.7	5	0.23	82.3	0	0
	$18MB_E$	84	0	84	0	252	11.5	18	0.56	110.2	0	0.60	92.3	0	0.79
	$18MB_M$	84	0	84	0	252	8.8	5	0.04	95.9	0	0.68	84.8	1	0.32
△ Murrumbidgee	$18MB_L$	84	0	84	0	252	10.0	27	0.25	90.2	4	0.24	84.7	0	0.52
	$17MV_E$	36	0	36	0	108	9.6	0	0.47	120.3	1	0.94	75.7	0	0.50
	$17MV_M$	45	0	45	0	135	10.3	1	0.38	117.9	0.00	0.65	68.7	1	0.36
	$17MV_L$	45	0	45	0	135	7.9	1	0.20	106.4	10	0.74	71.0	1	0.79
	$18MV_E$	84	84	0	0	168	9.6	10	0.41	124.0	17	0.44	75.6	0	0.61
	$18MV_M$	84	84	0	0	168	10.3	2	0.75	115.4	5	0.41	73.5	0	0.70
× Murray Valley	$18MV_L$	84	84	0	0	168	6.7	5	0.31	104.3	20	0.24	63.7	1	0.40
Overall	-	**291**	-	-	-	**2358**	**9.0**	**80**	**0.40**	**104.9**	**70**	**0.48**	**77.7**	**5**	**0.54**

*Each environment is a unique year-region-season combination.

Table 2: The multi-trait MET dataset, Part 2: Summary of agrnomic traits. Presented for grain yield (YLD), days to flowering (DTF) and plant height (PHT) is the minimum, mean and maximum for each year, region and season. Values presented are prior to scaling phenotypes to unit variance.

		YLD (t/ha)			DTF (days)			PHT (cm)		
		Min	Mean	Max	Min	Mean	Max	Min	Mean	Max
Year	2017	2.0	8.4	12.5	68.0	99.2	128.0	56.0	77.8	140.0
	2018	1.6	9.6	15.6	73.0	104.8	127.0	49.0	80.7	129.0
Region	△ Murrumbidgee	2.0	9.0	15.6	68.0	95.1	122.0	62.0	84.2	140.0
	× Murray Valley	1.6	9.0	12.5	86.0	114.7	128.0	49.0	71.2	99.0
Season	Early	2.0	10.5	15.6	99.0	116.4	128.0	65.0	83.6	129.0
	Mid	2.0	9.3	12.5	84.0	104.5	123.0	56.0	78.4	140.0
	Late	1.6	8.1	12.8	68.0	93.2	112.0	49.0	77.9	109.0

Table 3: Summary of the non-separable linear mixed models fitted to the multi-trait MET dataset. Presented is the number of estimated additive variance parameters, residual log-likelihood, AIC and percentage of variance explained across all traits ($\bar{v}_t$), environments ($\bar{v}_e$) and overall ($\bar{v}$).

Non-separable factor analytic linear mixed models						
Model	Params	Loglik	AIC	$\bar{v}_t$	$\bar{v}_e$	$\bar{v}$
diag*	36	3493.5	-6519.0	-	-	-
diag	36	3438.6	-6515.1	-	-	-
NFA1	72	3626.6	-6819.1	37.8	60.0	57.7
NFA2	107	3764.5	-7025.0	69.3	72.8	71.2
NFA3	**141**	**3820.3**	**-7068.5**	**86.2**	**86.8**	**87.1**
NFA4	174	3853.9	-7069.9	93.1	93.4	94.0

Note: 145 non-additive, non-genetic and residual variance parameters estimated in all models, except *diag** which includes a non-separable residual model with 198 parameters. The selected NFA3 model is distinguished with *bold font*.

Table 4: Summary of the **a.** unstructured and **b.** partially separable factor analytic linear mixed models fitted to the multi-trait MET dataset. Presented is the number of estimated trait and environmental variance parameters, residual log-likelihood, AIC and percentage of variance explained across all traits ($\bar{v}_t$), environments ($\bar{v}_e$) and overall ($\bar{v}$).

a. Unstructured factor analytic linear mixed models

Model	Params	Loglik	AIC	$\bar{v}_t$	$\bar{v}_e$	$\bar{v}$
diag:diag	2-12	3379.3	-6440.7	-	-	-
us:diag	5-12	3392.3	-6462.7	-	-	-
UFA1	8-12	3634.0	-6938.0	80.3	74.6	78.6
UFA2	**8-23**	**3661.4**	**-6970.9**	**83.3**	**78.1**	**81.5**
UFA3	8-33	3668.2	-6964.3	85.1	80.9	83.8

b. Partially separable factor analytic linear mixed models

Model	Params	Loglik	AIC	$\bar{v}_t$	$\bar{v}_e$	$\bar{v}$
SFA1-1	5-23	3571.4	-6796.6	32.9	51.8	53.4
SFA1-2	5-34	3579.4	-6790.7	33.3	52.9	54.9
SFA2-1	7-23	3639.8	-6929.5	54.4	57.9	60.6
SFA2-2	7-34	3648.7	-6925.4	55.6	60.3	63.9
SFA3-1	8-23	3667.4	-6982.7	68.1	72.7	76.1
SFA3-2	**8-34**	**3678.2**	**-6982.0**	**76.3**	**77.6**	**81.1**
SFA3-3	8-44	3685.3	-6976.4	77.4	79.8	82.8

Note: 145 non-additive, non-genetic and residual variance parameters estimated in all models. The selected UFA2 and SFA3-2 models are distinguished with *bold font*.

Table 5: The SFA3-2 model, Part 1: Summary of **a.** traits and **b.** environments. Presented is the REML estimates of additive genetic variance ($\bar{\mathbf{g}}_{\mathbf{t}}$ and $\bar{\mathbf{g}}_{\mathbf{e}}$), percentage of variance explained for individual traits and environments ($\mathbf{v_t}$ and $\mathbf{v_e}$) and the estimates of unrotated factor loadings ($\hat{\boldsymbol{\lambda}}_{\mathbf{t}_{l_t}}$ and $\hat{\boldsymbol{\lambda}}_{\mathbf{e}_{l_e}}$). The traits are grain yield (YLD), days to flowering (DTF) and plant height (PHT).

a. Traits	$\bar{\mathbf{g}}_{\mathbf{t}}$	$\mathbf{v_t}$	$\hat{\boldsymbol{\lambda}}_{\mathbf{t}_1}$	$\hat{\boldsymbol{\lambda}}_{\mathbf{t}_2}$	$\hat{\boldsymbol{\lambda}}_{\mathbf{t}_3}$
YLD	0.36	60.0	1	0	0
DTF	3.03	73.7	-0.08	3.21	0
PHT	16.06	95.3	-4.00	-2.07	7.10
Overall	**6.48**	**76.3**	-	-	-

b. Envs	$\bar{\mathbf{g}}_{\mathbf{e}}$	$\mathbf{v_e}$	$\hat{\boldsymbol{\lambda}}_{\mathbf{e}_1}$	$\hat{\boldsymbol{\lambda}}_{\mathbf{e}_2}$
$17MB_E$	11.88	92.2	0.66	0
$17MB_M$	4.94	74.3	0.36	0.17
$17MB_L$	2.43	69.9	0.27	0.10
$17MV_E$	4.55	47.5	0.30	0.04
$17MV_M$	5.77	85.0	0.40	0.22
$17MV_L$	5.61	83.8	0.34	0.28
$18MB_E$	14.25	89.4	0.63	0.30
$18MB_M$	5.14	60.0	0.36	0.04
$18MB_L$	7.70	83.2	0.42	0.29
$18MV_E$	3.21	75.6	0.24	0.24
$18MV_M$	6.54	86.6	0.41	0.26
$18MV_L$	5.75	84.2	0.39	0.22
Overall	**6.48**	**77.6**	-	-

Note: The overall additive genetic variance ($\bar{g}$) and the percentage of variance explained across all traits and environments ($\bar{v}_t$ and $\bar{v}_e$) is presented in the final row.

Table 6: The SFA3-2 model, Part 2: Additive genetic correlations between grain yield (YLD), days to flowering (DTF) and plant height (PHT) for each environment.

Env	YLD-DTF	YLD-PHT	DTF-PHT
$17MB_E$	-0.02	-0.42	-0.23
$17MB_M$	-0.02	-0.33	-0.18
$17MB_L$	-0.02	-0.29	-0.23
$17MV_E$	-0.01	-0.23	-0.09
$17MV_M$	-0.02	-0.38	-0.23
$17MV_L$	-0.02	-0.37	-0.21
$18MB_E$	-0.02	-0.41	-0.21
$18MB_M$	-0.01	-0.28	-0.12
$18MB_L$	-0.02	-0.37	-0.19
$18MV_E$	-0.02	-0.33	-0.23
$18MV_M$	-0.02	-0.38	-0.23
$18MV_L$	-0.02	-0.37	-0.23
Overall	**-0.02**	**-0.36**	**-0.20**

Table 7: The SFA3-2 model, Part 3: Summary of rice growing environments for **a.** grain yield (YLD), **b.** days to flowering (DTF) and **c.** plant height (PHT). Presented for each trait is the REML estimates of additive genetic variance ($\bar{\mathbf{g}}_{\mathbf{e}_i}$), percentage of variance explained for individual environments ($\mathbf{v}_{\mathbf{e}_i}$) and the rotated factor loadings ($\hat{\boldsymbol{\lambda}}^*_{i;l_e}$).

	a. YLD (t/ha)				**b.** DTF (days)				**c.** PHT (cm)			
Env	$\bar{\mathbf{g}}_{\mathbf{e}_1}$	$\mathbf{v}_{\mathbf{e}_1}$	$\hat{\boldsymbol{\lambda}}^*_{1;1}$	$\hat{\boldsymbol{\lambda}}^*_{1;2}$	$\bar{\mathbf{g}}_{\mathbf{e}_2}$	$\mathbf{v}_{\mathbf{e}_2}$	$\hat{\boldsymbol{\lambda}}^*_{2;1}$	$\hat{\boldsymbol{\lambda}}^*_{2;2}$	$\bar{\mathbf{g}}_{\mathbf{e}_3}$	$\mathbf{v}_{\mathbf{e}_3}$	$\hat{\boldsymbol{\lambda}}^*_{3;1}$	$\hat{\boldsymbol{\lambda}}^*_{3;2}$
$17MB_E$	0.56	77.5	0.60	-0.27	4.43	100.0	1.92	-0.86	30.66	99.2	-5.04	2.24
$17MB_M$	0.30	51.6	0.40	0.01	2.59	61.5	1.27	0.03	11.93	92.6	-3.32	-0.09
$17MB_L$	0.21	39.5	0.29	-0.02	0.87	100.0	0.93	-0.08	6.22	96.0	-2.44	0.20
$17MV_E$	0.30	31.4	0.29	-0.09	4.47	21.4	0.93	-0.28	8.89	72.6	-2.42	0.73
$17MV_M$	0.33	62.8	0.45	0.04	2.13	100.0	1.45	0.14	14.85	98.4	-3.80	-0.38
$17MV_L$	0.33	60.7	0.43	0.12	2.16	86.4	1.38	0.39	14.35	97.0	-3.61	-1.01
$18MB_E$	0.65	76.6	0.70	0.02	6.28	81.0	2.25	0.06	35.83	97.2	-5.90	-0.16
$18MB_M$	0.32	40.8	0.34	-0.11	4.05	32.4	1.09	-0.36	11.05	82.0	-2.86	0.93
$18MB_L$	0.41	63.3	0.50	0.10	3.55	71.1	1.61	0.31	19.14	95.2	-4.21	-0.80
$18MV_E$	0.24	47.6	0.31	0.12	1.16	100.0	1.01	0.38	8.22	97.1	-2.64	-1.01
$18MV_M$	0.36	65.6	0.48	0.07	2.42	100.0	1.54	0.24	16.85	98.6	-4.03	-0.63
$18MV_L$	0.33	62.2	0.45	0.04	2.20	100.0	1.44	0.13	14.73	98.4	-3.78	-0.34
Overall	**0.36**	**60.0**	**57.3**	**3.1**	**3.03**	**73.7**	**69.5**	**3.7**	**16.06**	**95.3**	**90.5**	**4.8**

Note: The overall additive genetic variance ($\bar{g}_{t_i}$), percentage of variance explained across all environments (v_{t_i}) and by individual rotated factors ($\mathbf{v}_i$) is presented in the final row.

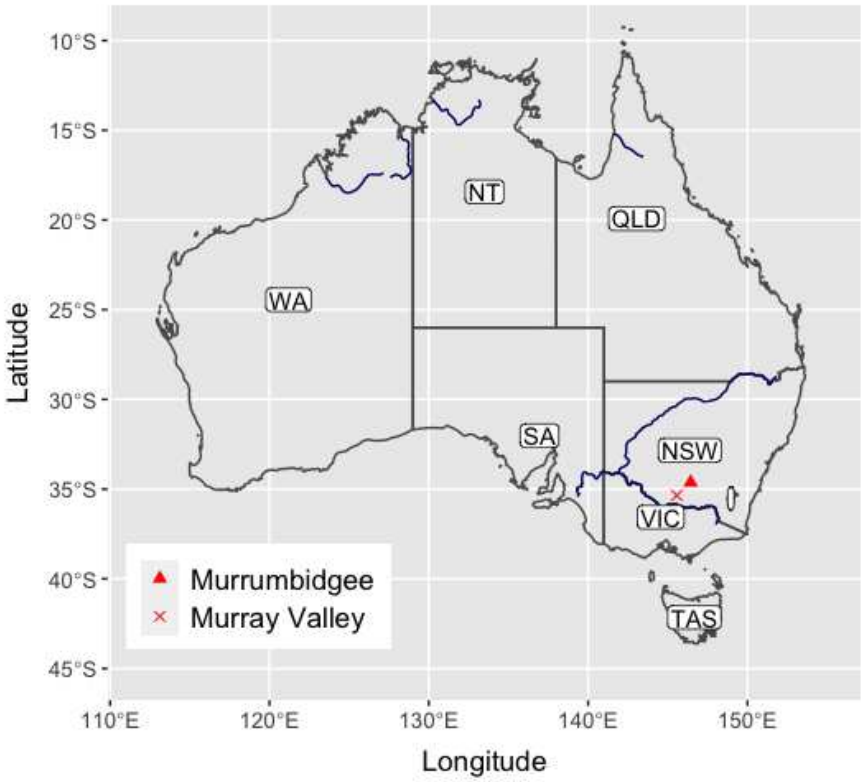

Fig. 1: Map of rice growing areas in the multi-trait MET dataset. Regions are distinguished by shape.

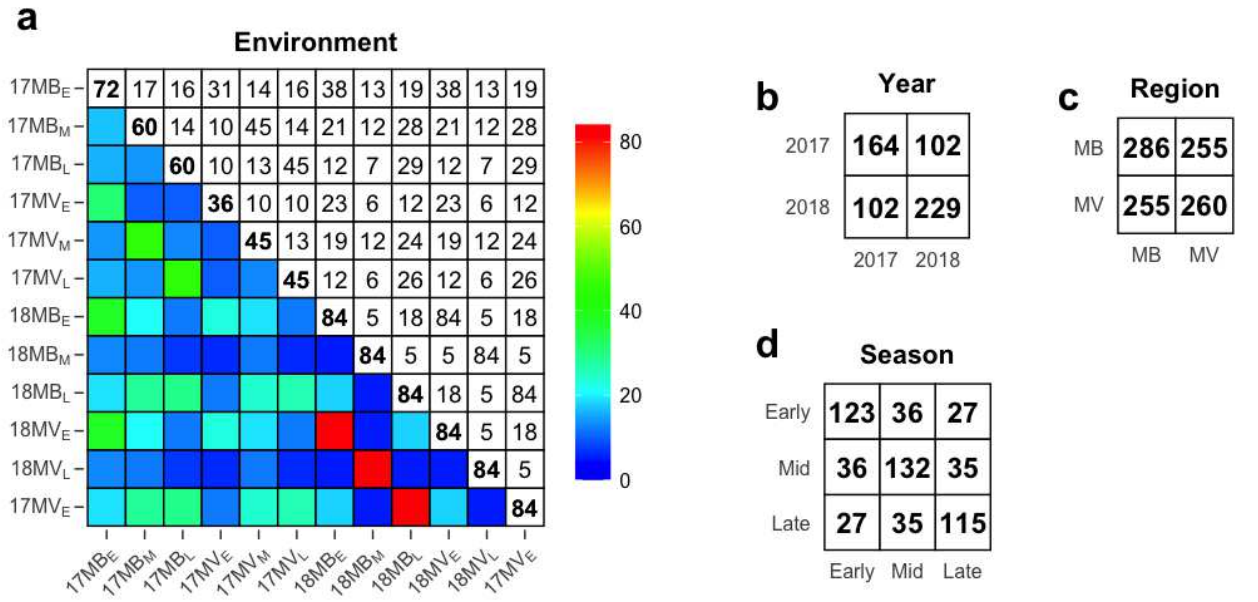

Fig. 2: Connectivity in the multi-trait MET dataset in terms of the number of genotypes in common between pairs of **a.** environments, **b.** years, **c.** regions and **d.** seasons. The diagonal elements in all figures represent the number of unique genotypes, while the lower diagonal in **a** is shown as a heatmap with supporting colorkey.

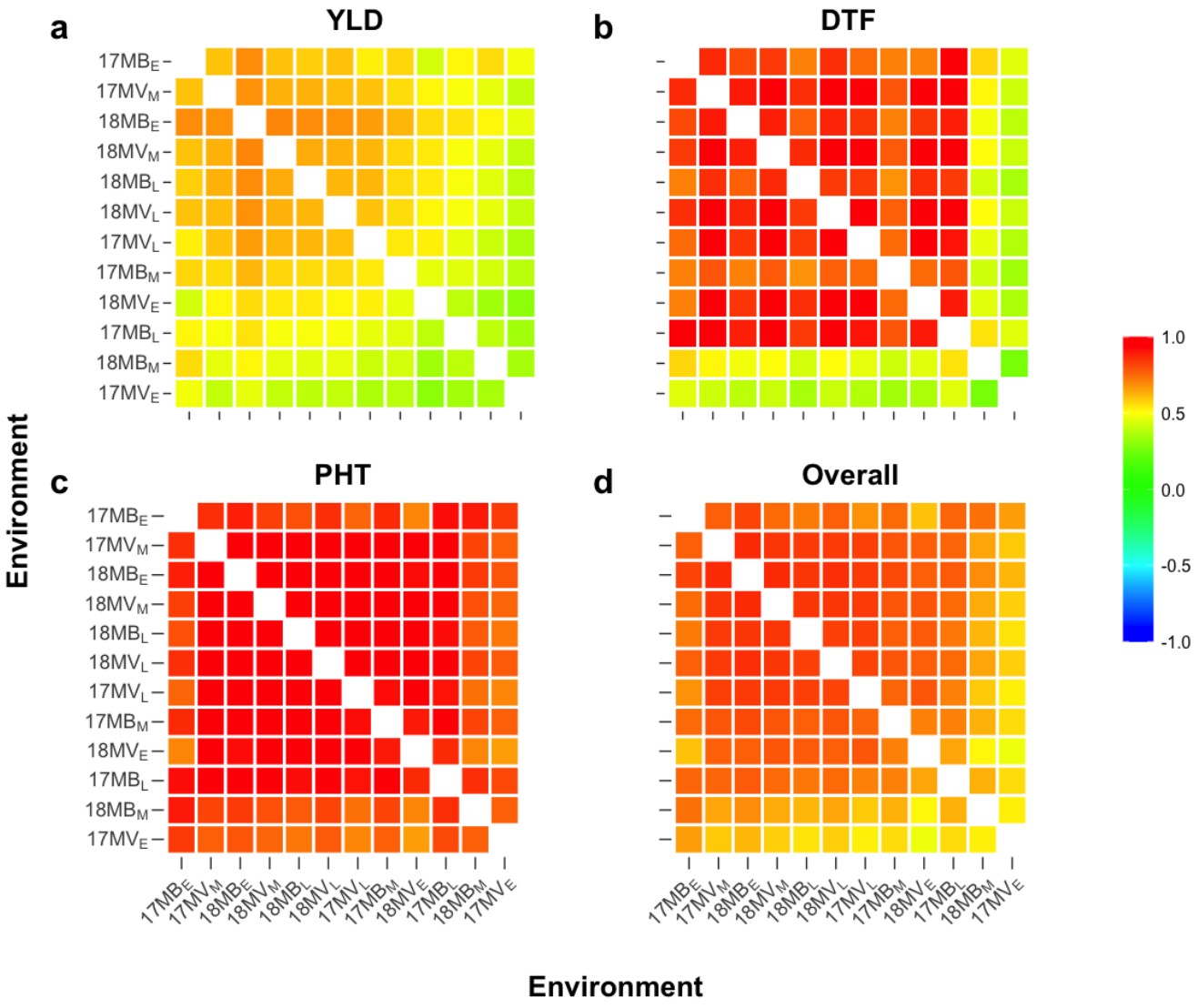

Fig. 3: Heatmaps of the additive genetic correlation matrices between rice growing environments for **a.** grain yield (YLD), **b.** days to flowering (DTF) and **c.** plant height (PHT) and **d.** overall. All matrices are ordered using the dendrogram applied to **a**. The colourkey ranges from 1 (agreement in rankings) through zero (dissimilarity in rankings) to -1 (reversal of rankings).

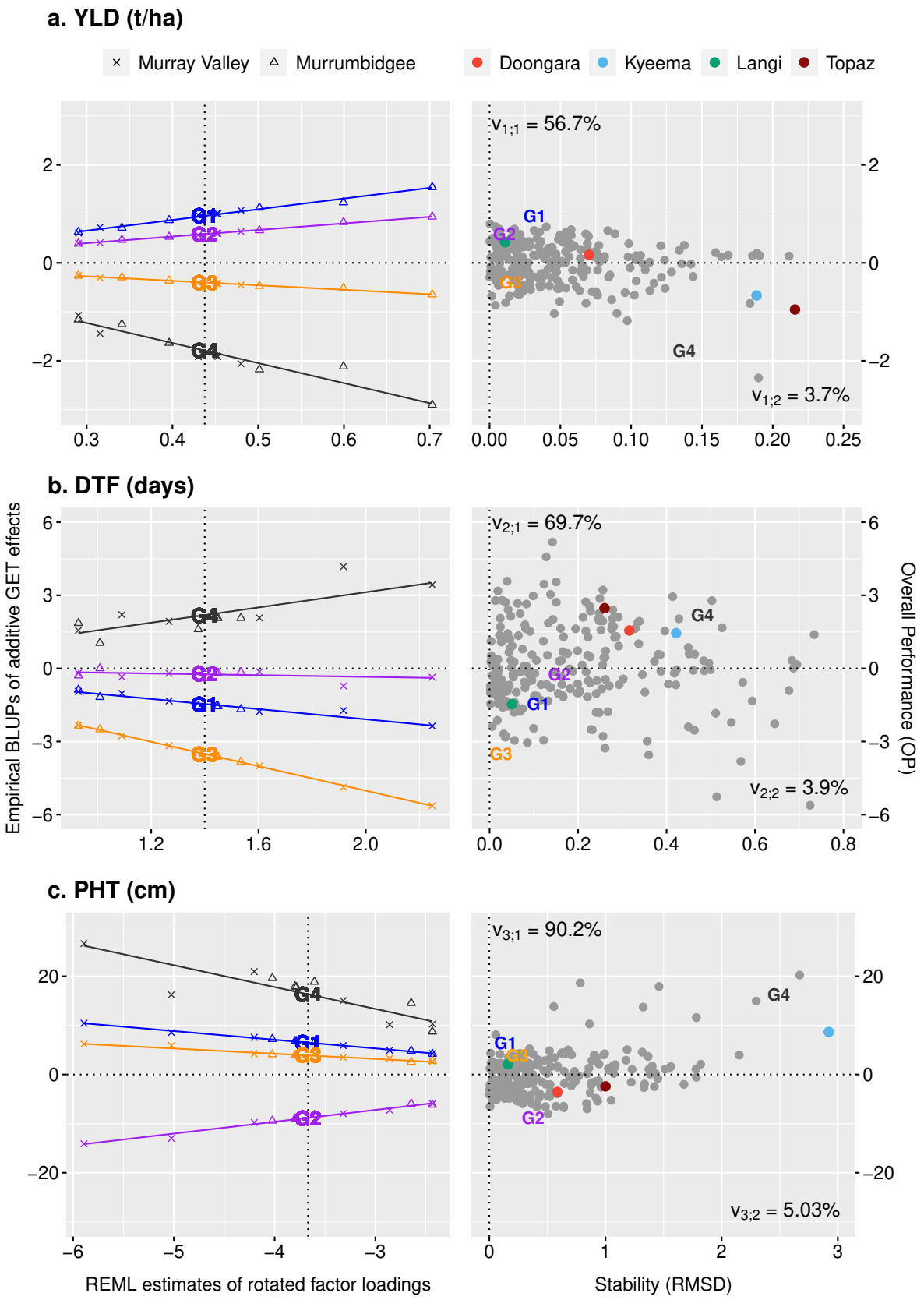

Fig. 4: Latent regression and OP vs RMSD plots for **a.** grain yield (YLD), **b.** days to flowering (DTF) and **c.** plant height (PHT). The latent regression plots are demonstrated using reference genotypes G1-G4 while the OP vs RMSD plots include all 262 test genotypes and four check cultivars. The labels on the latent regression plots represent the OP of G1-G4 taken at the mean loading of the first rotated factor (*vertical dotted line*). Growing regions are distinguished by *shape*. The variance explained by the first and second rotated factors ($v_{i;1}$ and $v_{i;2}$) is labelled on the OP vs RMSD plots. Values presented are after transforming parameters back to their original scale.

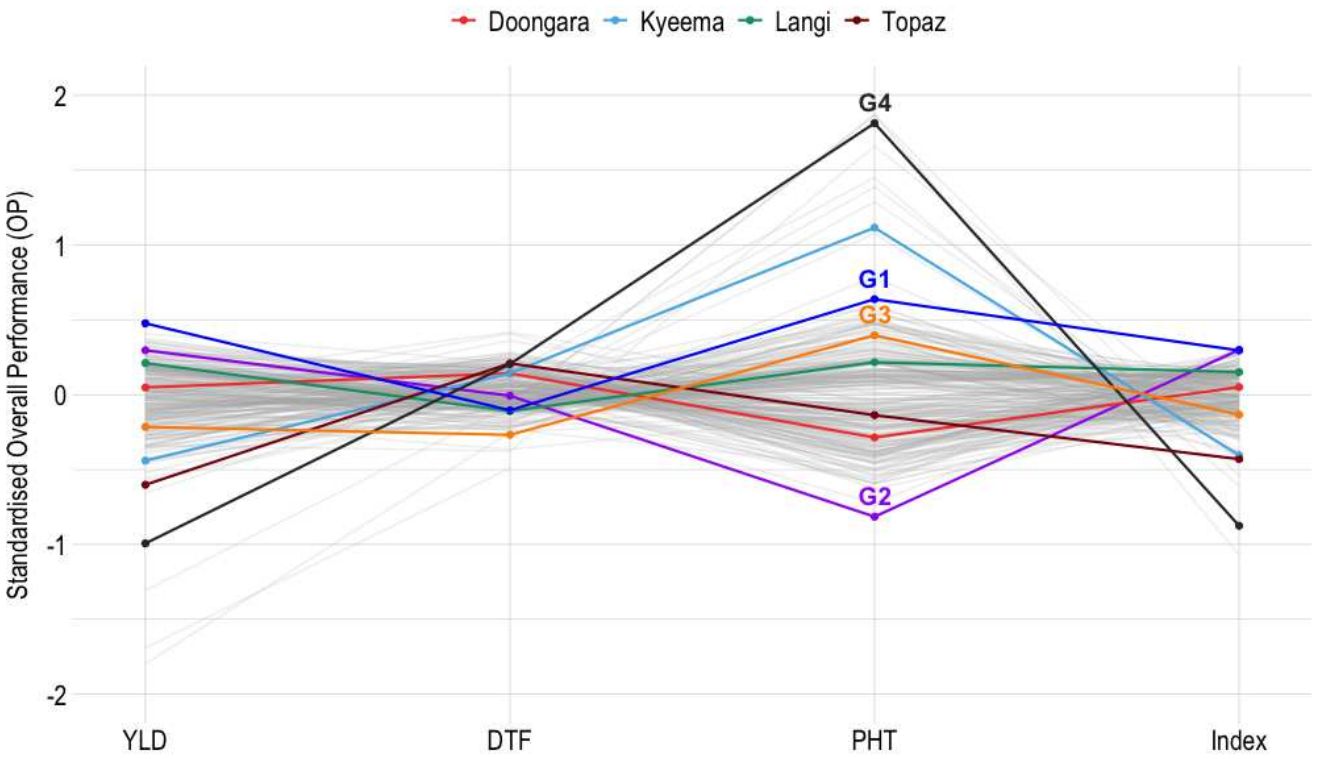

Fig. 5: Parallel coordinate plot with standardised OP for grain yield (YLD), days to flowering (DTF) and plant height (PHT) as well as the selection index. The weights used in the index are 0.7, -0.2 and -0.1 for YLD, DTF and PHT, respectively. The plot includes all 262 test genotypes and four check cultivars (distinguished by *colour*). The labels on the plot correspond to the reference genotypes G1-G4.

Appendix A Model Separability

This appendix demonstrates the difference between non-separable, separable and partially separable structures. The examples below are demonstrated using a environment by trait variance matrix, with s traits and p environments.

A.1 Non-separable models

Let $\mathbf{A}$ denote a general $ps \times ps$ *non-separable* trait by environment variance matrix. Consider $s = 2$ traits and $p = 2$ environments as an example, the non-separable variance matrix can therefore be written as:

$$\mathbf{A} = \begin{bmatrix} a_{11} & a_{11;12} & a_{11;21} & a_{11;22} \\ a_{12;11} & a_{12} & a_{12;21} & a_{12;22} \\ a_{21;11} & a_{21;12} & a_{21} & a_{21;22} \\ a_{22;11} & a_{22;12} & a_{22;21} & a_{22} \end{bmatrix},$$

where a_{ij} is the variance for the i^{th} trait and j^{th} environment combination, $a_{ij;kl}$ is the covariance between the i^{th} trait and j^{th} environment combination and the k^{th} trait and l^{th} environment combination. This variance matrix is non-separable since it cannot be represented by the Kronecker product of two matrices.

A.2 Separable models

When $\mathbf{A}$ has a *separable* structure, it can be written as the Kronecker product of two matrices. In this case, $\mathbf{A} = \mathbf{B} \otimes \mathbf{C}$, where $\mathbf{B}$ is a $s \times s$ variance matrix for traits, $\mathbf{C}$ is a $p \times p$ variance matrix for environments and $\otimes$ is the Kronecker product operator. The separable variance matrix can therefore be written as:

$$\begin{aligned} \mathbf{B} \otimes \mathbf{C} &= \begin{bmatrix} b_{11} & b_{12} \\ b_{21} & b_{22} \end{bmatrix} \otimes \begin{bmatrix} c_{11} & c_{12} \\ c_{21} & c_{22} \end{bmatrix} \\ &= \begin{bmatrix} b_{11}c_{11} & b_{11}c_{12} & b_{12}c_{11} & b_{12}c_{12} \\ b_{11}c_{21} & b_{11}c_{22} & b_{12}c_{21} & b_{12}c_{22} \\ b_{21}c_{11} & b_{21}c_{12} & b_{22}c_{11} & b_{22}c_{12} \\ b_{21}c_{21} & b_{21}c_{22} & b_{22}c_{21} & b_{22}c_{22} \end{bmatrix}, \end{aligned} \tag{36}$$

where $b_{ii}c_{jj}$ is the variance for the i^{th} trait and j^{th} environment combination, $b_{ij}c_{kl}$ is the covariance between the i^{th} trait and j^{th} environment combination and the k^{th} trait and l^{th} environment combination. Lastly, note that separable structures are favourable since they involve far fewer variance parameters than non-separable models as the number of traits and environments increase, that is $(p + s)$ parameters compared to ps parameters.

A.3 Partially separable models

When $\mathbf{A}$ has a *partially separable* structure, it can be written as $\mathbf{A} = \mathbf{B} \otimes \mathbf{C} + \mathbf{D}$, where $\mathbf{B}$ and $\mathbf{C}$ are defined above and $\mathbf{D}$ is a $ps \times ps$ diagonal variance matrix. The partially separable variance matrix can therefore be written as:

$$\mathbf{B} \otimes \mathbf{C} + \mathbf{D} = \begin{bmatrix} b_{11} & b_{12} \\ b_{21} & b_{22} \end{bmatrix} \otimes \begin{bmatrix} c_{11} & c_{12} \\ c_{21} & c_{22} \end{bmatrix} + \begin{bmatrix} d_{11} & 0 & 0 & 0 \\ 0 & d_{12} & 0 & 0 \\ 0 & 0 & d_{21} & 0 \\ 0 & 0 & 0 & d_{22} \end{bmatrix}$$

$$= \begin{bmatrix} b_{11}c_{11} + d_{11} & b_{11}c_{12} & b_{12}c_{11} & b_{12}c_{12} \\ b_{11}c_{21} & b_{11}c_{22} + d_{22} & b_{12}c_{21} & b_{12}c_{22} \\ b_{21}c_{11} & b_{21}c_{12} & b_{22}c_{11} + d_{33} & b_{22}c_{12} \\ b_{21}c_{21} & b_{21}c_{22} & b_{22}c_{21} & b_{22}c_{22} + d_{44} \end{bmatrix},$$

where $b_{ii}c_{jj}$ and $b_{ij}c_{kl}$ are defined in Equation 36 and d_{ij} is an additional variance for the i^{th} trait and j^{th} environment combination. Partially separable structures are favourable since they involve far fewer variance parameters than non-separable models and are less restrictive than completely separable models. This feature is demonstrated below.

A.4 Application to the SFAk model

The SFAk model is based on a three way separable structure, which is given by:

$$\begin{aligned} \mathbf{G_a} &= \mathbf{G_t} \otimes \mathbf{G_e} \otimes \mathbf{G_g} \\ &= (\mathbf{\Lambda_t}\mathbf{\Lambda_t}^\top + \mathbf{\Psi_t}) \otimes (\mathbf{\Lambda_e}\mathbf{\Lambda_e}^\top + \mathbf{\Psi_e}) \otimes \mathbf{G_g}, \end{aligned} \tag{37}$$

where $\mathbf{G_t}$ is a $s \times s$ factor analytic variance matrix between traits based on k_t factors, $\mathbf{G_e}$ is a $p \times p$ factor analytic variance matrix between environments based on k_e factors and $\mathbf{G_g}$ is the $v \times v$ genomic relationship matrix between genotypes. Note that the separable structure in Equation 37 is restrictive since it assumes the same genotype by environment interaction (GEI) pattern for each trait and the same genotype by trait interaction (GTI) pattern for each environment. This can be demonstrated using $s = 2$ traits and p environments, with:

$$\mathbf{G_a} = \begin{bmatrix} (\mathbf{\Lambda_{t_1}}\mathbf{\Lambda_{t_1}}^\top + \psi_{t_1}) & \mathbf{\Lambda_{t_1}}\mathbf{\Lambda_{t_2}}^\top \\ \mathbf{\Lambda_{t_2}}\mathbf{\Lambda_{t_1}}^\top & (\mathbf{\Lambda_{t_2}}\mathbf{\Lambda_{t_2}}^\top + \psi_{t_2}) \end{bmatrix} \otimes (\mathbf{\Lambda_e}\mathbf{\Lambda_e}^\top + \mathbf{\Psi_e}) \otimes \mathbf{G_g} \tag{38}$$

where $\mathbf{\Lambda}_{\mathbf{t}_i}^\top = (\lambda_{i;1}, \lambda_{i;2}, \ldots, \lambda_{i;k_t})^\top$ is a k_t-vector in which $\lambda_{i;l}$ is the i^{th} trait loading for the l^{th} latent factor, such that $\mathbf{\Lambda_t} = [\mathbf{\Lambda}_{\mathbf{t}_1}^\top \mathbf{\Lambda}_{\mathbf{t}_2}^\top \ldots \mathbf{\Lambda}_{\mathbf{t}_s}^\top]^\top$. The GEI pattern for each trait is the same, that is $(\mathbf{\Lambda_e}\mathbf{\Lambda_e}^\top + \mathbf{\Psi_e})$, which is scaled by $(\mathbf{\Lambda_{t_1}}\mathbf{\Lambda_{t_1}}^\top + \psi_{t_1})$ and $(\mathbf{\Lambda_{t_2}}\mathbf{\Lambda_{t_2}}^\top + \psi_{t_2})$ for traits 1 and 2, respectively. This also the case for the GTI pattern for each environment.

The partially separable factor analytic (SFAk) model is obtained by modifying Equation 38 to enable a different GEI pattern for each trait and a different GTI for each environment. This can also be demonstrated using $s = 2$ traits and p environments, with:

$$\mathbf{G_a} = \begin{bmatrix} \mathbf{\Lambda_{t_1}}\mathbf{\Lambda_{t_1}}^\top & \mathbf{\Lambda_{t_1}}\mathbf{\Lambda_{t_2}}^\top \\ \mathbf{\Lambda_{t_2}}\mathbf{\Lambda_{t_1}}^\top & \mathbf{\Lambda_{t_2}}\mathbf{\Lambda_{t_2}}^\top \end{bmatrix} \otimes \mathbf{\Lambda_e}\mathbf{\Lambda_e}^\top + \begin{bmatrix} \psi_{t_1} & 0 \\ 0 & \psi_{t_2} \end{bmatrix} \otimes \mathbf{I}_p + \begin{bmatrix} 1 & 0 \\ 0 & 1 \end{bmatrix} \otimes \mathbf{\Psi_e},$$

The GEI pattern for each trait is now different, that is $[\mathbf{\Lambda_{t_1}}\mathbf{\Lambda_{t_1}}^\top]\mathbf{\Lambda_e}\mathbf{\Lambda_e}^\top + \psi_{t_1}\mathbf{I}_p + \mathbf{\Psi_e}$ and $[\mathbf{\Lambda_{t_2}}\mathbf{\Lambda_{t_2}}^\top]\mathbf{\Lambda_e}\mathbf{\Lambda_e}^\top + \psi_{t_2}\mathbf{I}_p + \mathbf{\Psi_e}$ for traits 1 and 2, respectively. This also the case for the GTI pattern for each environment.

Appendix B Model identifiability

when $k > 1$, $[k_t(k_t-1) + k_e(k_e-1) + 2]/2$ constraints are required to ensure identifiability of $\mathbf{G}$ during estimation. There are three types of constraints required:

1. When $k_t \geq 1$, the $k_t(k_t-1)/2$ elements are constrained to zero in the upper right triangle of $\mathbf{\Lambda_t}$. The first element in the upper left is also constrained to one due to the separable parametrisation of $[\mathbf{\Lambda_t} \otimes \mathbf{\Lambda_e}]$.
2. When $k_e > 1$, the $k_e(k_e-1)/2$ elements are constrained in the upper right of $\mathbf{\Lambda_e}$.
3. One element in either $\mathbf{\Psi_t}$ or $\mathbf{\Psi_e}$ is constrained to zero since $\boldsymbol{\delta_t}$ and $\boldsymbol{\delta_e}$ are linear combinations of each other. Preliminary analysis revealed no residual additive variation specific to 18MV_E, so that $\psi_{e_{10}}$ was set to zero in all subsequent analyses.

There are also two constraints required to ensure identifiability of $\mathbf{R}$ during estimation:

1. The first element in the upper left of $\mathbf{R_t}$ is constrained to one due to the separable parametrisation of $\left[\mathbf{R_t} \otimes \mathbf{R_e}\right]$.
2. One element in either $\mathbf{\Sigma_t}$ or $\mathbf{\Sigma_e}$ is constrained to zero since the associated effects are linear combinations of each other. Preliminary analysis revealed no random error specific to DTF, so that $\sigma^2_{t_2}$ was set to zero in all subsequent analyses.